Since January 2020 Elsevier has created a COVID-19 resource centre with free information in English and Mandarin on the novel coronavirus COVID-19. The COVID-19 resource centre is hosted on Elsevier Connect, the company's public news and information website.

Results in Control and Optimization 9 (2022) 100176

Contents lists available at ScienceDirect

Results in Control and Optimization

journal homepage: www.elsevier.com/locate/rico

Optimal control strategies to combat COVID-19 transmission: A mathematical model with incubation time delay

Harendra Pal Singh [a], Sumit Kaur Bhatia [b,*], Yashika Bahri [b], Riya Jain [b]

[a] Cluster Innovation Centre, University of Delhi, Delhi, India
[b] AIAS, Amity University, Noida, India

ARTICLE INFO

MSC:
92B05
92D25
92D40

Keywords:
COVID-19
Epidemics
Basic reproduction number
Optimality
Sensitivity analysis
Delay

ABSTRACT

The coronavirus disease 2019, started spreading around December 2019, still persists in the population all across the globe. Though different countries have been able to cope with the disease to some extent and vaccination for the same has been developed, it cannot be ignored that the disease is still not on the verge of completely eradicating, which in turn creates a need for having deeper insights of the disease in order to understand it well and hence be able to work towards its eradication. Meanwhile, using mitigation strategies like non-pharmaceutical interventions can help in controlling the disease. In this work, our aim is to study the dynamics of COVID-19 using compartmental approach by applying various analytical methods. We obtain formula for important tools like R_0 and establish the stability of disease-free equilibrium point for $R_0 < 1$. Further, based on R_0, we discuss the stability and existence of the endemic equilibrium point. We incorporate various control strategies possible and using optimal control theory, study their expected positive impacts on the spread of the disease. Later, using a biologically feasible set of parameters, we numerically analyse the model. We even study the trend of the outbreak in China, for over 120 days, where the active cases rise up to a peak and then the curve flattens.

1. Introduction

Over the years, humankind has seen many epidemics. In addition to the loss of priceless lives, the economic, social and psychological pressure on people (and in general, on the entire world) are some examples of immediate impacts of any epidemic. History is full of such eras, where an epidemic lead to an economy's downfall. For instance, the deadly Spanish Flu of 1918, which lasted for about two years, infected approximately 500 million people on the planet, resulted in around 20–50 million casualties [1] and led to a GDP loss of 11%, 15% and 17% in USA, Canada and UK, respectively [2]. The epidemic came to an end only because of the development of a natural herd immunity, however, no proper medication or vaccination could be developed to cope with it. Some diseases persist in the population for a very long time and cannot be eradicated for decades. For instance, the HIV/AIDS epidemic started in the year 1981 and the disease is still spreading among people with approximately 37.9 million cases as of 2018 [3]. There is no cure for the disease till date, however, with treatment an infected person can lead a long-healthy life, but there is no way to stop this disease from spreading other than taking some preventive measures. With the development of research and medicine, humankind has also successfully eradicated some epidemics in the past. The most iconic example is that of eradicating the Smallpox disease, which was said to have lasted for around 3000 years. The epidemic was brought under control by mass vaccination [4].

* Corresponding author.
E-mail addresses: harendramaths@gmail.com (H.P. Singh), sumit2212@gmail.com (S.K. Bhatia), yashikabahri20@gmail.com (Y. Bahri), jain.ria1997@gmail.com (R. Jain).

https://doi.org/10.1016/j.rico.2022.100176
Received 10 July 2022; Received in revised form 24 August 2022; Accepted 28 September 2022
Available online 3 October 2022

One of the current epidemics is Coronavirus Disease 2019 (COVID-19), which is caused by Severe Acute Respiratory Syndrome Coronavirus 2 (SARS-CoV-2). The infection was first detected in Wuhan, China in December 2019, when it was thought to be an infectious disease transmitted from animals to humans. But the World Health Organization and Chinese authorities soon announced in January 2020 that it could spread from person to person. With the first confirmed case in December 2019, as of 14 August 2022, the global number has risen to approximately 595.3 million cases with approximately 6.4 million deaths. Although, as of 14 August 2022, we also have approximately 568.8 million recovered cases, but the number of active cases globally still fall around 20 million [5]. There is no denying with the fact that a major proportion of infected individuals will not get severely infected and will also recover quickly but considering the massive death tolls, the virus cannot be taken lightly. Even though mankind has made advances in medicine and treatment, it takes a lot of time to come up with a proper treatment for a newly identified disease. However, mathematical modelling is data-driven and hence can be used to understand any epidemic. Epidemiologists compile real perspectives on the disease in a mathematical model and use real data to estimate the extent of transmission as well as various measures with which the disease can be brought under control in the short and long term. For instance, in [6] Ochoche et al. used a simple SIR model to understand the spread of Measles. Similarly, in [7] Olivia et al. used an $SAIR$ compartmental model to study seasonal and H1N1 influenza. Several other models on different diseases such as HIV, Hepatitis B virus, HBV and HCV co-infections have been formulated by many authors [8–13].

We can also find a lot of literature where models have been formulated and studied for COVID-19 by many authors [14–35]. Pang el al. [17] constructed an SEIHR model to characterize transmission dynamics, which was then used to match published data on confirmed cases in Wuhan. DDEs (delay differential equations) appear frequently in research and engineering applications. Introduction of time delays in a model has lead to a better understanding of more complicated structures [36–38]. The model's resilience and accuracy are improved by adding a time delay. Though some SEIR and SEIRJ models address latency, the latent E is supposed to be weakly contagious. As a result, these models are unable to describe the properties of a new coronavirus that can be transmitted throughout the incubation phase. COVID-19's transmission dynamics with an incubation delay are investigated by the authors in [39–44]. Other system delays may need to be addressed in order to properly forecast the outcome of the models. During the first wave of COVID-19 in the United States, the delay in the effect of restricting community mobility on the spread of the virus was explored in [45].

In a dynamical system, optimum command of a mathematical model helps in predicting, forecasting, estimating, or identifying the ideal scenario for eradicating a disease. Vaccination is very useful while attempting to control a disease. Vaccines for COVID-19 have been developed and people are being vaccinated in many countries all over the globe. Bur we also have examples of countries, like the United Kingdom, United States of America, France, Germany, India, etc., that faced a new wave of COVID-19 even after the vaccination programme had started. Under such circumstances, control strategies turn out to be useful in controlling the disease. Right now, precautionary measures, government interventions, improved medical facilities, societal limitation on a huge scale, tracking of contacts, large-scale testing, identification and treatment of cases, face mask, sanitizer, etc., can be considered as useful and notable control strategies. Motivated by this some researchers [22,46–58] studied the optimal policies that could be employed to control COVID-19. Our goal is to study the outcome when we impose some restrictions on the susceptible class and provide medical help to infectious class. After taking these steps, it can be said that either disease will eliminate or will spread slowly in the population. Suggestions provided through analysis and simulation done with help of mathematical modelling become a powerful tool for general well-being.

Several compartmental system for the outbreak of COVID-19 have been constructed since last year. Authors in [17] have developed SEIHR model where they have not considered asymptomatic and quarantine classes. Authors in [16] consider SIRD model following law of mass action and their model does not incorporate exposed, asymptomatic class. In [19], [20] authors consider compartmental model with standard incidence rate without hospitalized and quarantine class respectively. In [59] authors studied SIHRS model and have not included exposed, asymptomatic class. Authors in [60] do not include asymptomatic and quarantine classes in their model. In [18] authors, constructed a COVID-19 SEIQR difference-equation model. We have tried to build a comprehensive model which incorporates seven compartments, symptomatic, exposed, asymptomatic, infected, quarantine, hospitalized and recovered, time delay which is over and above the incubation period and control strategies as well. Also, our model incorporates rate of bilinear incidence(βSI) and saturated rate of occurrence ($\beta SI/(1+\alpha I)$), which captures the inhibitory behaviour of susceptible class to infected individuals with symptoms, which as per our knowledge is not considered as yet.

The uniqueness of this paper lies in the complexity of the model. We formulate a compartmental model with 7 compartments, trying to incorporate all movements possible. Introducing a delay parameter along with the control parameters, adds up to this. Cases have been recorded where some recovered individuals have been tested positive again in China [61] as well as Hong Kong [62]. Therefore, it is important to consider the possibility of recovery not implying permanent immunity in the recovered individuals, which is being taken care of in the model. Furthermore, we have done both the analytical as well as the numerical analysis of the model. Then, we compare our results with the actual numbers from China. The importance of incorporating the delay parameter, which takes into account the extra days over the incubation period (2–14 days) for the symptoms to be visible, lies with the fact that this delay makes it very difficult to protect the susceptible class from the infected individuals or provide the necessary treatment at the initial stages. Although, a lot of researches have been conducted using delay parameters [36,63–66], still the effect of this parameter on COVID-19 is not explored much. Therefore, we have attempted to study what effects incubation period can have on the spread of the disease by combining it with several control strategies.

In this study, we formulate a new model equipped with delay and control parameters, which we use to model COVID-19 epidemic. In Section 1, we give a brief introduction about the model and Section 2 deals with model formulation. We have examined the dynamics of a non-delayed system in Section 3 wherein we have discussed the existence and stability of the equilibrium points.

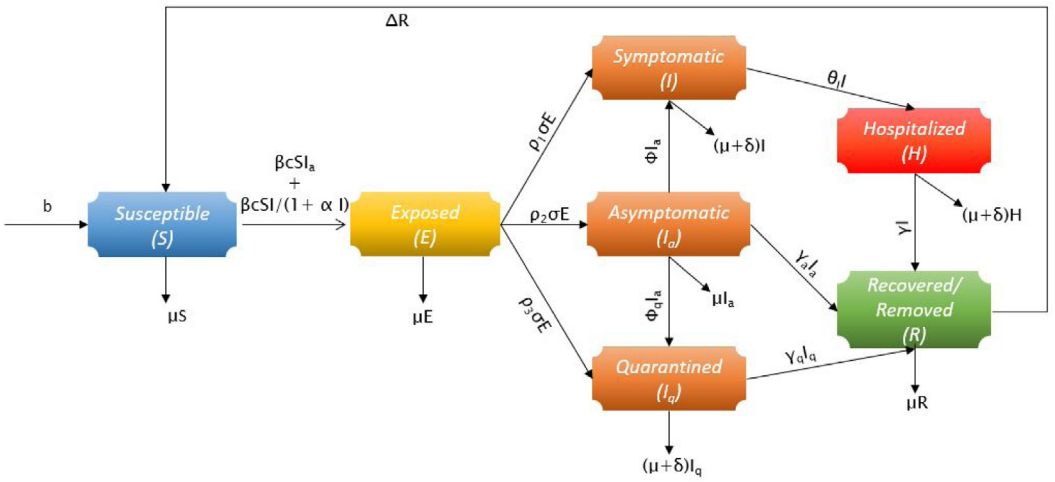

Fig. 1. Flow diagram of the model.

The dynamics of a delayed system is examined in Section 4 wherein the stability of the equilibrium points and the sensitivity of basic reproduction number have been discussed. In Section 5, we have studied the impact of control strategies. Section 6 includes numerical analysis of the COVID-19 model and comparing it to real time data of China. We have then concluded the paper in Section 7, summarizing the results and our findings along with a few strategies, highlighting the importance of non-pharmaceutical interventions.

2. Model formulation

Now, we begin the formulation of our model. Our aim is to come up with a mathematical model that can capture the real aspect of the COVID-19 disease, as much as possible. We have based our model on the compartmental modelling approach, where change in each compartment is denoted by an ordinary differential equation. To begin, we assume that the entire population (N) at any time can be split into seven compartments as can be seen in Fig. 1. This also means that at any time, the population of all the seven compartments add up to the total population at that time. Further, the population may decrease when individuals in any compartment die naturally (at a rate μ) or due to COVID-19 (at a rate δ) and may increase due to the recruitment of susceptible individuals (at a rate b). Next, we also assume that initially the entire population is at a risk of getting infected, i.e., everyone is susceptible to the disease. These susceptible individuals will move to the exposed compartment after they come in contact with an infected individual.

While modelling transmissible diseases, it is very important to use an appropriate rate of incidence in order to make accurate predictions. Authors frequently use a bilinear incidence rate βSI, which is based on the law of mass action. βSI suggests that the number of infectives increase linearly without a bound, which seems odd when the symptoms of the disease are well identifiable (because when symptoms are well identifiable the behaviour of susceptible class changes). In [67], Capasso and Serio used a non-linear saturated incidence rate $\frac{\beta SI}{1+\alpha I}$, where βI is the force of infection and $\frac{1}{1+\alpha I}$ measures the inhibition effect due to the change in behaviour of the susceptible individuals when I is large. Such an incidence rate ensures that $\frac{\beta I}{1+\alpha I}$ tends to a saturation level of $\frac{\beta}{\alpha}$, i.e., the increase in the number of infected individuals is not unbounded. In view of the above discussion, we take the incidence rate as $\beta cSI_a + \frac{\beta cSI}{1+\alpha I}$, where c is the contact rate and β is the probability of transmission per contact. This is justified because the asymptomatic individuals do not show any symptoms, therefore, there is no inhibition towards disease transmission. On the other hand, symptomatic individuals are identifiable, which leads to a behavioural change of susceptible class leading to the inhibition effect.

After the mean incubation period (σ^{-1}), the E individuals go to infection classes I, I_a and I_q in proportions ρ_1, ρ_2 and ρ_3, respectively. Individuals having severe symptoms after σ^{-1} days go in the I class, individuals showing no symptoms after σ^{-1} days go to I_a class and individuals having very mild symptoms after σ^{-1} days home isolate themselves and move to I_q class. In general, quarantined individuals are those people that home isolate themselves as a precautionary measure because they doubt that they might be infected (probably because they met an infected person recently and are now showing very mild symptoms). Similarly, we have a movement from 'Asymptomatic' compartment to the 'Quarantined' compartment in order to acknowledge those asymptomatic individuals who home isolate themselves as a precautionary measure (because they might have come in contact someone who was later diagnosed as COVID-positive). Since I_q and I_a individuals have only mild symptoms or no symptoms at all, we assume that they naturally recover under home isolation and move directly to the 'Recovered' compartment. And lastly, since symptomatic individuals are adversely affected they move to the 'Hospitalized' compartment (i.e., seek treatment), and post recovery move to 'Recovered' compartment. We assume that any individual moving to the 'Hospitalized' compartment is already diagnosed as positive for COVID-19.

Since we are still new to the COVID-19 disease we cannot be completely sure if recovery from the disease provides permanent immunity. Motivated by this, we incorporate parameter $\triangle$ in the model that denotes the rate at which the recovered individuals become susceptible again. Consistent with the above description the model has been described with the help of a flow diagram in Fig. 1. Although, in reality the movement from one stage to another is a much more complex process, we have aimed to keep the model as realistic as possible, while ensuring it still can be mathematically solved and interpreted. Combining everything that we have discussed above, we formulate the following system of seven ordinary differential equations that represent our model mathematically:

$$\begin{aligned}
\frac{dS}{dt} &= b - \beta c S I_a - \frac{\beta c S I}{1+\alpha I} - \mu S + \triangle R,\\
\frac{dE}{dt} &= \beta c S I_a + \frac{\beta c S I}{1+\alpha I} - (\sigma+\mu)E,\\
\frac{dI}{dt} &= \rho_1 \sigma E + \phi I_a(t) - (\theta_I + \mu + \delta)I,\\
\frac{dI_a}{dt} &= \rho_2 \sigma E - (\phi_q + \gamma_a + \mu)I_a - \phi I_a(t),\\
\frac{dI_q}{dt} &= \rho_3 \sigma E + \phi_q I_a - I_q(\gamma_q + \delta + \mu),\\
\frac{dH}{dt} &= \theta_I I - H(\gamma + \delta + \mu),\\
\frac{dR}{dt} &= I_a\gamma_a + \gamma H - R(\triangle + \mu) + I_q\gamma_q.
\end{aligned} \tag{2.1}$$

As discussed earlier, it is known that sometimes it can take a few days more than the incubation period of 2–14 days [68–73] for the COVID-19 symptoms to be visible. Therefore, individuals that were identified as asymptomatic because they did not show any symptoms after σ^{-1} days can actually turn out to be symptomatic after a delay and hence there is a movement from 'Asymptomatic' compartment to 'Symptomatic' compartment. Thus, we incorporate a delay parameter τ which takes into account this delay in the development of symptoms in infected individuals. Thus, the time delayed model is as follows:

$$\begin{aligned}
\frac{dS}{dt} &= b - \beta c S I_a - \frac{\beta c S I}{1+\alpha I} - \mu S + \triangle R,\\
\frac{dE}{dt} &= \beta c S I_a + \frac{\beta c S I}{1+\alpha I} - (\sigma+\mu)E,\\
\frac{dI}{dt} &= \rho_1 \sigma E + \phi I_a(t-\tau) - (\theta_I + \mu + \delta)I,\\
\frac{dI_a}{dt} &= \rho_2 \sigma E - (\phi_q + \gamma_a + \mu)I_a - \phi I_a(t-\tau),\\
\frac{dI_q}{dt} &= \rho_3 \sigma E + \phi_q I_a - I_q(\gamma_q + \delta + \mu),\\
\frac{dH}{dt} &= \theta_I I - H(\gamma + \delta + \mu),\\
\frac{dR}{dt} &= I_a\gamma_a + \gamma H - R(\triangle + \mu) + I_q\gamma_q.
\end{aligned} \tag{2.2}$$

Consider the initial conditions for system (2.2) are of the form:

$S(\eta) = f_1(\eta)$, $E(\eta) = f_2(\eta)$, $I(\eta) = f_3(\eta)$, $I_a(\eta) = f_4(\eta)$, $I_q(\eta) = f_5(\eta)$, $H(\eta) = f_6(\eta)$, $R(\eta) = f_7(\eta)$; where, $f_i(\eta) \in C([-\tau, 0], \mathbb{R}^7_+)$, which is a Banach space of continuous functions from $[-\tau, 0]$ into $\mathbb{R}^7_+$; such that, $f_i(\eta) \geq 0$ for $\eta \in [-\tau, 0)$, and $f_i(0) > 0$, $\forall\ i = 1, 2, 3, 4, 5, 6, 7$. Table 1 briefly describes all the parameters of the model.

3. Dynamics of non-delayed system (2.1)

3.1. Positivity and boundedness of solutions

For system (2.1) to be biologically meaningful, it is required that the solutions with positive initial data are positive and bounded for all $t \geq 0$, as the state variables in system (2.1) represent populations.

Now, as done by Naresh et al. in [74], using a theorem on differential inequalities [75], it can be easily shown that,

$$\begin{aligned}
&\frac{dS}{dt} \geq -(\beta c I_a + \frac{\beta c I}{1+\alpha I} + \mu)S,\\
\implies\ &S(t) \geq S(0)\ exp\{-(\beta c I_a + \frac{\beta c I}{1+\alpha I} + \mu)t\} > 0,
\end{aligned}$$

Thus, $S(t) > 0$ for all $t > 0$. Then on similar line, we can show that $E(t) > 0$, $I(t) > 0$, $I_a(t) > 0$, $I_q(t) > 0$, $H(t) > 0$ and $R(t) > 0$.

Further, adding all the equations in (2.1):

$$\begin{aligned}
\frac{dN}{dt} =& b - \mu N - \delta(I + I_q + H),\\
\leq& b - \mu N.
\end{aligned}$$

Table 1
Description of model parameters.

Parameter	Description
b	Recruitment of susceptible class
μ	Natural death rate
δ	Disease-induced death rate
ρ_1	Fraction of individuals that become symptomatic after getting exposed
ρ_2	Fraction of individuals that become asymptomatic after getting exposed
ρ_3	Fraction of individuals that get quarantined after getting exposed
α	Parameter that captures inhibition of Susceptible individuals
c	Contacts per unit time
β	Probability of transmission per contact
σ	Rate at which exposed individuals become infected
θ_I	Rate at which symptomatic individuals get hospitalized
γ	Rate at which symptomatic individuals recover
γ_a	Rate at which asymptomatic individuals recover
γ_q	Rate at which Quarantined individuals recover
ϕ	Rate at which asymptomatic individuals start showing symptoms
ϕ_q	Rate of quarantine of asymptomatic individuals
Δ	Rate at which Recovered individuals loose immunity
τ	Delay parameter measuring delay in development of symptoms in asymptomatic class

Simplifying and solving the above differential equation we get,

$N = (S + E + I + I_a + I_q + H + R) \leq \frac{b}{\mu} + Ce^{-\mu t}$.

Clearly, as $t \to \infty$ it can be seen that $N = (S + E + I + I_a + I_q + H + R) \to \frac{b}{\mu}$. Hence, the solution for system (2.1) is bounded. Therefore, solution space, $\{(S, E, I, I_a, I_q, H, R) \in \mathbb{R}^7_+ : 0 < N \leq \frac{b}{\mu}\}$ is positively invariant.

In the next sections, we have attempted to interpret the model analytically as well as numerically.

3.2. Basic reproduction number (R_0)

In this section, we discuss about important analytical tools required for stability analysis: like the basic reproduction number (R_0) and disease-free equilibrium points. Disease-free equilibrium point can be thought of as that equilibrium position where there is no trace of infection in the population, i.e., the point where the disease no longer persists in the population. Proceeding as in Section 3 of [76], the DFE (E_0) of system (2.1) can be easily computed by setting RHS of each equation in (2.1) equal to zero.

$$E_0 = \left(\frac{b}{\mu}, 0, 0, 0, 0, 0, 0\right). \tag{3.1}$$

Basic reproduction number is an epidemiological term used for the mean number of individuals turning into infectives in a susceptible population due to one infected individual existing in it. R_0 has an important role to play in epidemiology, because it determines important factors, like whether the disease will remain in the population or will it be eliminated. In general, we can say if $R_0 < 1$ then the disease will be eradicated eventually otherwise it will persist. Although there are a variety of methods that can be employed to calculate R_0, in this paper we make use of the next generation matrix method [6,51] to come to a formula (3.2).

Step 1: To begin, we use the notation $\mathcal{X}$ for system (2.1) as follows:

$$\mathcal{X} = (E, I, I_a, I_q, H, R, S).$$

Which can be rewritten as,

$$\begin{aligned}\mathcal{X}' &= \mathcal{Y}(x) - \mathcal{Z}(x),\\ &= \mathcal{Y}(x) - [\mathcal{Z}^-(x) - \mathcal{Z}^+(x)],\end{aligned}$$

where, $\mathcal{Y}(x) = \left[y_{k1}\right]_{7X1}$ is such that $y_{11} = \beta c S(I_a + \frac{I}{1+\alpha I})$ and every other element in this column vector is zero. Further, each element of this vector corresponds to a group of terms resulting in new infectious individuals in each of the seven classes; and

$$\mathcal{Z}(x) = \begin{bmatrix} E(\mu+\sigma) \\ I(\theta_I + \delta + \mu) - E\rho_1\sigma - I_a\phi \\ I_a(\mu + + \gamma_a + \phi_q + \phi) - E\rho_2\sigma \\ I_q(\gamma_q + \mu + \delta) - E\rho_3\sigma - I_a\phi_q \\ H(\gamma + \delta + \mu) - I\theta_I \\ R\,\Delta - I_q\gamma_q - H\gamma + R\mu - I_a\gamma_a \\ \beta c S(I_a + \frac{I}{I\alpha+1}) + S\mu - b - R\,\Delta \end{bmatrix}, \text{ is a collection of left over terms.}$$

Step 2: Next step is to find the Jacobian matrices of $\mathscr{Y}(x)$ and $\mathscr{Z}(x)$ at DFE, which are as mentioned below: $D\mathscr{Y}(E_0) = \begin{bmatrix} F & 0 \\ 0 & 0 \end{bmatrix}$ and $D\mathscr{Z}(E_0) = \begin{bmatrix} V & 0 \\ J_1 & J_2 \end{bmatrix}$,
where,

$$F = \begin{bmatrix} 0 & \frac{b\beta c}{\mu} & \frac{b\beta c}{\mu} & 0 \\ 0 & 0 & 0 & 0 \\ 0 & 0 & 0 & 0 \\ 0 & 0 & 0 & 0 \end{bmatrix}, \qquad V = \begin{bmatrix} (\sigma+\mu) & 0 & 0 & 0 \\ -\sigma\rho_1 & (\theta_I+\delta+\mu) & -\phi & 0 \\ -\sigma\rho_2 & 0 & (\mu+\phi+\gamma_a+\phi_q) & 0 \\ -\sigma\rho_3 & 0 & -\phi_q & (\gamma_q+\mu+\delta) \end{bmatrix},$$

$$J_1 = \begin{bmatrix} 0 & -\theta_I & 0 & 0 \\ 0 & 0 & -\gamma_a & -\gamma_q \\ 0 & \beta bc\mu^{-1} & \beta bc\mu^{-1} & 0 \end{bmatrix}, \qquad J_2 = \begin{bmatrix} (\gamma+\mu+\delta) & 0 & 0 \\ -\gamma & (\mu+\Delta) & 0 \\ 0 & -\Delta & \mu \end{bmatrix}.$$

Step 3: Now, we compute next generation matrix which is defined as follows:

$$FV^{-1} = \begin{bmatrix} \frac{\beta bc\sigma}{\mu(\sigma+\mu)}\left(\frac{\rho_1}{(\theta_I+\mu+\delta)} + \frac{\rho_2\phi}{(\theta_I+\mu+\delta)(\phi+\phi_q+\gamma_a+\mu)} + \frac{\rho_2}{(\phi+\phi_q+\gamma_a+\mu)}\right) & \frac{\beta bc}{\mu(\theta_I+\mu+\delta)} & \frac{\beta bc}{\mu(\phi+\phi_q+\gamma_a+\mu)}\left(\frac{\phi}{(\delta+\theta_I+\mu)}+1\right) & 0 \\ 0 & 0 & 0 & 0 \\ 0 & 0 & 0 & 0 \\ 0 & 0 & 0 & 0 \end{bmatrix},$$

Finally, R_0 is computed by finding the spectral radius of FV^{-1} and is expressed mathematically as follows:

$$R_0 = \frac{\beta bc\sigma}{\mu\sigma+\mu^2}\left(\frac{\rho_1}{\mu+\theta_I+\delta} + \frac{\rho_2\phi(\mu+\phi+\gamma_a+\phi_q)^{-1}}{\theta_I+\delta+\mu} + \frac{\rho_2}{\gamma_a+\phi+\mu+\phi_q}\right). \tag{3.2}$$

3.3. Local stability of disease free equilibrium point

Here, we discuss the conditions required for local stability of the disease-free equilibrium point based on the basic reproduction number obtained in the previous subsection and state a theorem for the same.

The characteristic equation corresponding to Disease-Free Equilibrium point is as follows:

$$\begin{aligned} &-(\lambda+\mu)(\lambda+\Delta+\mu)(\lambda+\gamma+\mu+\delta)(\gamma_q+\mu+\delta+\lambda)(-\beta cS^*[\rho_1\sigma(\phi_q+\gamma_a+\mu+\lambda+\phi) \\ &\quad + \phi\rho_2\sigma] + (\theta_I+\mu+\delta+\lambda)[(\sigma+\mu+\lambda)(\phi_q+\gamma_a+\mu+\lambda+\phi) - \beta c\rho_2\sigma S^*]) = 0. \end{aligned}$$

Clearly, the four eigen values corresponding to the first four roots of the above equation are negative. The remaining three eigen values can be obtained from the following characteristic equation:

$$\begin{aligned} &-\beta cS^*[\rho_1\sigma(\phi_q+\gamma_a+\mu+\lambda+\phi) + \phi\rho_2\sigma] \\ &\quad + (\theta_I+\mu+\delta+\lambda)[(\sigma+\mu+\lambda)(\phi_q+\gamma_a+\mu+\lambda+\phi) - \beta c\rho_2\sigma S^*] = 0, \end{aligned} \tag{3.3}$$

which can be rewritten as,

$$f(\lambda) = (\lambda^3 + a_2\lambda^2 + a_1\lambda + a_0) + (c_2\lambda^2 + c_1\lambda + c_0) = 0, \tag{3.4}$$

where,

$$\begin{aligned} a_2 &= \theta_I + 3\mu + \phi_q + \delta + \gamma_a + \sigma, \\ a_1 &= -\beta c\sigma S^*\rho_1 - \beta c\sigma S^*\rho_2 + (\sigma+\mu)\{\theta_I + 2\mu + \gamma_a + \delta + \phi_q\} + (\theta_I+\mu+\delta)(\phi_q+\gamma_a+\mu), \\ a_0 &= -\beta c\sigma S^*(\phi_q\rho_1 + \rho_1\gamma_a + \mu\rho_1) + (\theta_I+\mu+\delta)\{-\beta c\sigma S^*\rho_2 + \sigma(\phi_q+\gamma_a+\mu) + \mu(\phi_q+\gamma_a+\mu)\}, \\ c_2 &= \phi, \\ c_1 &= \phi[2\mu+\sigma+\theta_I+\delta], \\ c_0 &= [(\sigma\phi+\phi\mu)(\theta_I+\delta+\mu) - \beta c\sigma S^*(\rho_1+\rho_2)]. \end{aligned}$$

Further, $a_0 + c_0$ can be simplified as follows:

$$a_0 + c_0 = (\sigma\theta_I + \sigma\mu + \sigma\delta + \mu\theta_I + \mu^2 + \mu\delta)(\phi_q + \phi + \gamma_a + \mu)(1 - R_0). \tag{3.5}$$

It can be observed from Eqs. (3.4) and (3.5) that, $f(0) = a_0 + c_0 < 0$ for $R_0 > 1$ and $\lim_{s\to\infty} f(s) = \infty$. This means that Eq. (3.4) has a positive real root and hence disease-free equilibrium is unstable for $R_0 > 1$.

Using Routh–Hurwitz criteria Eq. (3.4) will have roots with negative real part if the following conditions are satisfied:

C1 : $(a_0 + c_0) > 0$, $(a_1 + c_1) > 0$, $(a_2 + c_2) > 0$, and $(a_2 + c_2)(a_1 + c_1) > (a_0 + c_0)$.

Using Eq. (3.5), the first condition in **(C1)** is satisfied if $R_0 < 1$. Similarly, it can be shown that second, third and fourth conditions in **(C1)** are satisfied if $R_0 < 1$. Hence, we have the following theorem.

Theorem 1. *The disease-free equilibrium point of system (2.1) is locally asymptotically stable if* $R_0 < 1$.

3.4. Endemic equilibrium (E_1)

In this subsection, we find endemic equilibrium point (E_1) for (2.1). Let, E_1 of our system be as follows:

$$E_1 = (S^{**}, E^{**}, I^{**}, I_a^{**}, I_q^{**}, H^{**}, R^{**}). \tag{3.6}$$

Also let,

$$\lambda^{**} = \beta c I_a^{**} + \beta c \frac{I^{**}}{1 + \alpha I^{**}}. \tag{3.7}$$

To find the endemic equilibrium point ($S^{**}, E^{**}, I^{**}, I_a^{**}, I_q^{**}, H^{**}, R^{**}$), set RHS in each equation in (2.1) equal to 0, and solve for each compartment one by one.

To obtain an expression for S^{**}, set RHS of first equation in (2.1) equal to 0,

$$(\mu + \lambda^{**})S^{**} = b + \triangle R^{**}.$$

Substituting the value of R^{**} from Eq. (3.14) in the above expression, we get,

$$(\mu + \lambda^{**})S^{**} = b + \frac{\triangle \sigma A \lambda^{**} S^{**}}{BF}\left(\gamma_a \rho_2 + \frac{\gamma_q L}{D} + \frac{\gamma \theta_I G}{CP}\right),$$

$$\boldsymbol{S^{**} = \frac{b}{J\lambda^{**} + \mu}},$$

where,

$$\boldsymbol{J = 1 - \frac{\triangle \sigma A}{BF}\left(\gamma_a \rho_2 + \frac{\gamma_q L}{D} + \frac{\gamma \theta_I G}{CP}\right)}. \tag{3.8}$$

To obtain an expression for E^{**}, set RHS of second equation in (2.1) equal to 0. Solving for E^{**} we get,

$$\boldsymbol{E^{**} = A\lambda^{**} S^{**}},$$

where,

$$\boldsymbol{A = \frac{1}{(\mu + \sigma)}}. \tag{3.9}$$

To obtain an expression for I^{**}, set RHS of third equation in (2.1) equal to 0. Solving for I^{**} we get,

$$I^{**} = \frac{\rho_1 \sigma E^{**} + \phi I_a^{**}}{(\theta_I + \mu + \delta)}.$$

Substituting E^{**} and I_a^{**} from (3.9) and (3.11), respectively, in the above expression, we get,

$$\boldsymbol{I^{**} = \frac{\sigma A G \lambda^{**} S^{**}}{BC}},$$

where,

$$\begin{aligned} \boldsymbol{C} &= \boldsymbol{(\theta_I + \mu + \delta)}, \\ \boldsymbol{G} &= \boldsymbol{B\rho_1 + \phi\rho_2}. \end{aligned} \tag{3.10}$$

To obtain an expression for I_a^{**}, set RHS of fourth equation in (2.1) equal to 0. Solving for I_a^{**} we get,

$$I_a^{**} = \frac{\rho_2 \sigma E^{**}}{(\phi + \phi_q + \gamma_a + \mu)}.$$

Substituting E^{**} from Eq. (3.9) in the above expression, we get,

$$\boldsymbol{I_a^{**} = \frac{\rho_2 \sigma A \lambda^{**} S^{**}}{B}},$$

where,

$$\boldsymbol{B = (\phi + \phi_q + \gamma_a + \mu)}. \tag{3.11}$$

To obtain an expression for I_q^{**}, set RHS of fifth equation in (2.1) equal to 0. Solving for I_q^{**} we get,

$$I_q^{**} = \frac{\rho_3 \sigma E^{**} + \phi_q I_a^{**}}{(\gamma_q + \mu + \delta)}.$$

Substituting E^{**} and I_a^{**} from (3.9) and (3.11), respectively, in the above expression, we get,

$$I_q^{**} = \frac{\sigma A\lambda^{**}S^{**}}{DB}(B\rho_3 + \phi_q\rho_2),$$
$$\boldsymbol{I_q^{**} = \frac{\sigma AL\lambda^{**}S^{**}}{BD}},$$

where,

$$\boldsymbol{D = (\gamma_q + \mu + \delta)},$$
$$\boldsymbol{L = (B\rho_3 + \phi_q\rho_2)}. \tag{3.12}$$

To obtain an expression for H^{**}, set RHS of sixth equation in (2.1) equal to 0. Solving for H^{**}, we get,

$$H^{**} = \frac{\theta_I I^{**}}{(\gamma + \mu + \delta)}.$$

Substituting the value of I^{**} from Eq. (3.10) in the above expression, we get,

$$\boldsymbol{H^{**} = \frac{\theta_I\sigma AG\lambda^{**}S^{**}}{BCP}},$$

where,

$$\boldsymbol{P = (\gamma + \mu + \delta)}. \tag{3.13}$$

To obtain an expression for R^{**}, set RHS of last equation in (2.1) equal to 0. Solving for R^{**} we get,

$$R^{**} = \frac{\gamma_a I_a^{**} + \gamma_q I_q^{**} + \gamma H^{**}}{(\triangle + \mu)}.$$

Substituting the values of I_a^{**}, I_q^{**} and H^{**} from Eqs. (3.11), (3.12) and (3.13), respectively, in the above expression, we get,

$$R^{**} = \frac{\gamma_a\rho_2\sigma A\lambda^{**}S^{**}}{BF} + \frac{\gamma_q\sigma AL\lambda^{**}S^{**}}{DBF} + \frac{\gamma\theta_I\sigma AG\lambda^{**}S^{**}}{BCPF},$$
$$\boldsymbol{R^{**} = \frac{\sigma A\lambda^{**}S^{**}}{BF}\left(\gamma_a\rho_2 + \frac{\gamma_q L}{D} + \frac{\gamma\theta_I G}{CP}\right)},$$

where,

$$\boldsymbol{F = (\mu + \triangle)}. \tag{3.14}$$

Now, substituting the values of I^{**} and I_a^{**} from Eqs. (3.10) and (3.11) respectively, into Eq. (3.7) we have,

$$\lambda^{**} = \beta c I_a^{**} + \beta c\frac{I^{**}}{1 + \alpha I^{**}},$$
$$\lambda^{**} = \frac{\beta c\rho_2\sigma A\lambda^{**}S^{**}}{B} + \frac{\frac{\beta c\sigma AG\lambda^{**}S^{**}}{BC}}{1 + \frac{\alpha\sigma AG\lambda^{**}S^{**}}{BC}},$$
$$1 = \frac{\beta c\rho_2\sigma AS^{**}}{B} + \frac{\beta c\sigma AGS^{**}}{BC + \alpha\sigma AG\lambda^{**}S^{**}},$$
$$B[BC + \alpha\sigma AG\lambda^{**}S^{**}] = \beta c\rho_2\sigma AS^{**}[BC + \alpha\sigma AG\lambda^{**}S^{**}] + \beta c\sigma ABGS^{**},$$
$$B^2C + \alpha\sigma ABG\lambda^{**}S^{**} = \beta c\rho_2\sigma ABCS^{**} + \alpha\beta c\rho_2\sigma^2A^2G\lambda^{**}S^{**2} + \beta c\sigma ABGS^{**}.$$

Substituting the value of S^{**} from Eq. (3.8) in the above expression, we have,

$$B^2C + \alpha\sigma ABG\lambda^{**}\left(\frac{b}{\mu + J\lambda^{**}}\right) = \frac{\beta c\rho_2\sigma bABC}{\mu + J\lambda^{**}} + \frac{\alpha\beta c\rho_2\sigma^2b^2A^2G\lambda^{**}}{(\mu + J\lambda^{**})^2} + \frac{\beta c\sigma bABG}{\mu + J\lambda^{**}},$$
$$\left(B^2CJ + \alpha\sigma ABGb - \frac{\alpha\beta c\rho_2\sigma^2b^2A^2G}{\mu + J\lambda^{**}}\right)\lambda^{**} = \beta c\rho_2\sigma bABC + \beta c\sigma bABG - \mu B^2C.$$

Simplifying further we get,

$$\begin{aligned}(B^2CJ(\mu + J\lambda^{**}) + \alpha\sigma bABG(\mu + J\lambda^{**}) - \alpha\beta c\rho_2\sigma^2b^2A^2G)\lambda^{**} &= (\mu + J\lambda^{**})[\beta c\rho_2\sigma bABC + \beta c\sigma bABG - \mu B^2C] \\ &= (\mu + J\lambda^{**})\mu B^2C\left[\frac{\beta c\rho_2\sigma bA}{\mu B} + \frac{\beta c\sigma bAG}{\mu BC} - 1\right] \\ &= (\mu + J\lambda^{**})\mu B^2C\left[\left(\frac{\beta c\sigma bA}{\mu B}\right)\left(\rho_2 + \frac{G}{C}\right) - 1\right] \\ &= (\mu + J\lambda^{**})\mu B^2C\left[\left(\frac{\beta c\sigma bA}{\mu BC}\right)(C\rho_2 + G) - 1\right].\end{aligned}$$

Substituting value of G from Eq. (3.10), in the above expression, we have,

$$(B^2CJ(\mu + J\lambda^{**}) + \alpha\sigma bABG(\mu + J\lambda^{**}) - \alpha\beta c\rho_2\sigma^2 b^2A^2G)\lambda^{**} = (\mu + J\lambda^{**})\mu B^2C\left[\left(\frac{\beta c\sigma bA}{\mu BC}\right)(B\rho_1 + [C + \phi]\rho_2) - 1\right].$$

Substituting value of A, B and C from Eq. (3.9), (3.10) and (3.11) respectively, in the above expression, we have,

$$(B^2CJ(\mu+J\lambda^{**}) + \alpha\sigma bABG(\mu + J\lambda^{**}) - \alpha\beta c\rho_2\sigma^2 b^2A^2G)\lambda^{**} = (\mu + J\lambda^{**})\mu B^2C(R_0 - 1),$$

$$(B^2CJ(\mu+J\lambda^{**}) + \alpha\sigma bABG(\mu + J\lambda^{**}) - \alpha\beta c\rho_2\sigma^2 b^2A^2G)\frac{\lambda^{**}}{\mu B^2C} = (\mu + J\lambda^{**})(R_0 - 1).$$

Simplifying the above expression we get,

$$a_0\lambda^{**2} + b_0\lambda^{**} + c_0, \tag{3.15}$$

where,

$$a_0 = \frac{J^2}{\mu} + \frac{\alpha\sigma bAJG}{\mu BC},$$

$$b_0 = J + \frac{\alpha\sigma bAG}{BC} - \frac{\alpha\beta c\sigma^2\rho_2 b^2A^2G}{\mu B^2G} - J(R_0 - 1),$$

$$c_0 = -\mu(R_0 - 1).$$

It is interesting to observe that, with respect to every positive solution of λ^{**} in (3.15) we have a corresponding solution for $E_1 = (S^{**}, E^{**}, I^{**}, I_a^{**}, I_q^{**}, H^{**}, R^{**})$. Hence, there are as many endemic equilibria of (2.1) as there are positive roots of (3.15).

Looking at Eq. (3.15), we can observe that a_0 is always greater than 0 whereas c_0 is greater than 0 when R_0 is less than 1 and c_0 is less than 0 when R_0 is greater than 1. With the help of Descartes' rule of signs, the below theorem has been obtained for the existence of E_1.

Theorem 2. *The system (2.1) has:*

1. *a unique endemic equilibrium, if $c_0 < 0$ (i.e. $R_0 > 1$).*
2. *a unique endemic equilibrium, if $b_0 < 0$, and $c_0 = 0$ (i.e. $R_0 = 1$) or ${b_0}^2 - 4a_0c_0 = 0$.*
3. *exactly two endemic equilibria, if $c_0 > 0$ (i.e. $R_0 < 1$), $b_0 < 0$ and ${b_0}^2 - 4a_0c_0 > 0$.*

Remark: $R_0 < 1$ is not a sufficiency condition to eradicate any disease. Extra efforts are required.

3.5. Local stability of endemic equilibrium point

Here, we talk about the conditions required for the endemic equilibrium point to be locally stable. We have used *MATLAB* to obtain the characteristic equation of the Jacobian matrix at Endemic Equilibrium point (E_1) which is:

$$\lambda^7 + p_6\lambda^6 + p_5\lambda^5 + p_4\lambda^4 + p_3\lambda^3 + p_2\lambda^2 + p_1\lambda + p_0 + [q_6\lambda^6 + q_5\lambda^5 + q_4\lambda^4 + q_3\lambda^3 + q_2\lambda^2 + q_1\lambda + q_0] = 0, \tag{3.16}$$

where, $p_0, \ldots, p_6$ and $q_0, \ldots, q_6$ are listed in Appendix.

Using Routh–Hurwitz criterion the roots of Eq. (3.16) have negative real parts if and only if $|H_n'| > 0$ for $n = 1, \ldots, 7$, where for each n, H_n' is a Hurwitz matrix of order $n * n$, with general form:

$$H_n' = \begin{bmatrix} q_6 + p_6 & 1 & 0 & 0 & \ldots & 0 \\ q_4 + p_4 & q_5 + p_5 & q_6 + p_6 & 1 & \ldots & 0 \\ q_2 + p_2 & q_3 + p_3 & q_4 + p_4 & q_5 + p_5 & \ldots & 0 \\ \vdots & \vdots & \vdots & \vdots & \ddots & \vdots \\ 0 & 0 & 0 & 0 & 0 & q_{7-n} + p_{7-n} \end{bmatrix}, \tag{3.17}$$

with $p_j + q_j = 0$ if $j > 6$ or $j < 0$.

Thus, we have the following theorem.

Theorem 3. *Let E_1 be an endemic equilibrium point of system (2.1). Then, E_1 is locally asymptotically stable iff for each of the seven Hurwitz matrices defined as in Eq. (3.17), $|H_n'| > 0$.*

4. Dynamics of delayed system (2.2)

The positivity of system (2.2) can be proved on similar line as done in [77] and the boundedness of system (2.2) can be proved in a similar manner as in Section 3.1.

4.1. Equilibrium points and its stability

As mentioned by Tipsri and Chinviriyasit [78], the equilibrium solutions are same for the system with and without time delay. Therefore, to obtain the equilibrium points, we use $\tau = 0$. Hence, the Disease-Free and Endemic Equilibrium points of the system (2.2) are the same as obtained in Sections 3.1 and 3.4 respectively.

4.2. Local stability of disease free equilibrium point

In this subsection we will discuss stability of the system (2.2) around disease free equilibrium point.

When $\tau \neq 0$

The characteristic equation corresponding to the disease free equilibrium point E_0 is :

$$-(\lambda+\mu)(\lambda+\triangle+\mu)(\lambda+\gamma+\mu+\delta)(\gamma_q+\mu+\delta+\lambda)(-\beta c S^*[\rho_1\sigma(\phi_q+\gamma_a+\mu+\lambda+\phi e^{-\lambda\tau}) + \phi\rho_2\sigma e^{-\lambda\tau}] + (\theta_I+\mu+\delta+\lambda)[(\sigma+\mu+\lambda)(\phi_q+\gamma_a+\mu+\lambda+\phi e^{-\lambda\tau}) - \beta c\rho_2\sigma S^*]) = 0.$$

Clearly, the four eigen values corresponding to the first four roots of the above equation are negative. The remaining three eigen values can be obtained from the following characteristic equation:

$$f(\lambda) = (\lambda^3 + a_2\lambda^2 + a_1\lambda + a_0) + e^{-\lambda\tau}(c_2\lambda^2 + c_1\lambda + c_0) = 0, \tag{4.1}$$

where the coefficient $a_i's$ and $c_i's$ are same as obtained in Section 3.3.

For $\tau > 0$, Eq. (4.1) is a transcendental characteristic equation and the roots will be of the form, $\lambda = \eta(\tau) + \iota\omega(\tau)$, where $\omega > 0$. As explained by Mukandavire [79], the roots of a transcendental equation will have positive real parts if and only if it has purely imaginary roots. We will aim to obtain the conditions for which no such purely imaginary root exists for Eq. (4.1). These conditions will be then sufficient to conclude that all the roots of Eq. (4.1) for $\tau > 0$ have negative real parts.

Consider, $\lambda = \iota\omega$ $(\omega > 0)$ is a purely imaginary root of Eq. (4.1). Then, Eq. (4.1) becomes,

$$(-\iota\omega^3 - a_2\omega^2 + a_1\iota\omega + a_0) + [\cos(\omega\tau) - \iota\sin(\omega\tau)](-c_2\omega^2 + c_1\iota\omega + c_0) = 0.$$

Separating real–imaginary parts,

$$-a_2\omega^2 + a_0 + c_1\omega\sin(\omega\tau) - (c_2\omega^2 - c_0)\cos(\omega\tau) = 0,$$

$$-\omega^3 + a_1\omega + (c_2\omega^2 - c_0)\sin(\omega\tau) + c_1\omega\cos(\omega\tau) = 0.$$

Squaring both sides of the above two equations and adding we get,

$$\omega^6 + (-2a_1 + a_2^2 + c_2^2)\omega^4 + (a_1^2 - 2a_0a_2 + 2c_0c_2 - c_1^2)\omega^2 + (a_0^2 - c_0^2) = 0.$$

Taking $s = \omega^2$ we have:

$$s^3 + (-2a_1 + a_2^2 + c_2^2)s^2 + (a_1^2 - 2a_0a_2 + 2c_0c_2 - c_1^2)s + (a_0^2 - c_0^2) = 0. \tag{4.2}$$

If we assume that,

$$\textbf{C2}: (-2a_1 + a_2^2 + c_2^2) > 0,\ (a_1^2 - 2a_0a_2 + 2c_0c_2 - c_1^2) > 0,\ (a_0^2 - c_0^2) > 0, \text{ and } (-2a_1 + a_2^2 + c_2^2)(a_1^2 - 2a_0a_2 + 2c_0c_2 - c_1^2) > (a_0^2 - c_0^2)$$

then by Routh–Hurwitz criterion the roots for Eq. (4.2) will have negative real parts. However, there does not exist ω such that $s = \omega^2$ is negative. This poses a contradiction. Hence, whenever the conditions in **(C2)** are true, there does not exist a purely imaginary root of the transcendental Eq. (4.1). Hence, we have the following theorem.

Theorem 4. *Let, $R_0 < 1$ then for $\tau \geq 0$, the disease-free equilibrium point of system (2.2) is locally asymptotically stable if conditions in **(C1)** and **(C2)** are satisfied. Also, the disease-free equilibrium point of system (2.2) is unstable for $R_0 > 1$.*

Now, we will obtain the condition for stability of the Endemic Equilibrium point.

4.3. Local stability of endemic equilibrium point

When $\tau \neq 0$.

The characteristic equation corresponding to endemic equilibrium point (E_1) is as follows:

$$\lambda^7 + p_6\lambda^6 + p_5\lambda^5 + p_4\lambda^4 + p_3\lambda^3 + p_2\lambda^2 + p_1\lambda + p_0 + e^{-\lambda\tau}[q_6\lambda^6 + q_5\lambda^5 + q_4\lambda^4 + q_3\lambda^3 + q_2\lambda^2 + q_1\lambda + q_0] = 0, \tag{4.3}$$

where, $p_0, \ldots, p_6$ and $q_0, \ldots, q_6$ are listed in Appendix. For $\tau > 0$, Eq. (4.3) is a transcendental characteristic equation and the roots will be of the form, $\lambda = \eta(\tau) + \iota\omega(\tau)$, where $\omega > 0$. As done previously for local stability of E_0, we will aim to obtain the conditions for which no purely imaginary root exists for Eq. (4.3). Let if possible, Eq. (4.3) have a purely complex root of the form: $\lambda = \iota\omega$.

Then, Eq. (4.3) becomes:

$$
\begin{aligned}
&(-\imath\omega^7 - p_6\omega^6 + \imath p_5\omega^5 + p_4\omega^4 - \imath p_3\omega^3 - p_2\omega^2 + \imath p_1\omega + p_0)\\
&+ [\cos(\omega\tau) - \imath\sin(\omega\tau)](-q_6\omega^6 + \imath q_5\omega^5 + q_4\omega^4 - \imath q_3\omega^3 - q_2\omega^2 + \imath q_1\omega + q_0) = 0,\\
&\Rightarrow [(-p_6\omega^6 + p_4\omega^4 - p_2\omega^2 + p_0) + \imath(-\omega^7 + p_5\omega^5 - p_3\omega^3 + p_1\omega)]\\
&\quad + [\cos(\omega\tau) - \imath\sin(\omega\tau)][(-q_6\omega^6 + q_4\omega^4 - q_2\omega^2 + q_0) + \imath(q_5\omega^5 - q_3\omega^3 + q_1\omega)] = 0,\\
&\Rightarrow (-p_6\omega^6 + p_4\omega^4 - p_2\omega^2 + p_0) + \imath(-\omega^7 + p_5\omega^5 - p_3\omega^3 + p_1\omega)\\
&\qquad + (-q_6\omega^6 + q_4\omega^4 - q_2\omega^2 + q_0)\cos(\omega\tau) + (q_5\omega^5 - q_3\omega^3 + q_1\omega)\sin(\omega\tau)\\
&\qquad + \imath[(q_5\omega^5 - q_3\omega^3 + q_1\omega)\cos(\omega\tau) + (q_6\omega^6 - q_4\omega^4 + q_2\omega^2 - q_0)\sin(\tau\omega)] = 0.
\end{aligned}
$$

Separating real–imaginary parts:

$$
\begin{aligned}
Real: &-(q_6\omega^6 - q_4\omega^4 + q_2\omega^2 - q_0)\cos(\omega\tau) + (q_5\omega^5 - q_3\omega^3 + q_1\omega)\sin(\omega\tau)\\
&= (p_6\omega^6 - p_4\omega^4 + p_2\omega^2 - p_0),\\
Complex: &(q_5\omega^5 - q_3\omega^3 + q_1\omega)\cos(\omega\tau) + (q_6\omega^6 - q_4\omega^4 + q_2\omega^2 - q_0)\sin(\omega\tau)\\
&= (\omega^7 - p_5\omega^5 + p_3\omega^3 - p_1\omega).
\end{aligned}
\tag{4.4}
$$

Squaring both sides of the above two equations and adding we get:

$$
\begin{aligned}
&(q_6\omega^6 - q_4\omega^4 + q_2\omega^2 - q_0)^2 + (q_5\omega^5 - q_3\omega^3 + q_1\omega)^2\\
&\qquad = (p_6\omega^6 - p_4\omega^4 + p_2\omega^2 - p_0)^2 + (\omega^7 - p_5\omega^5 + p_3\omega^3 - p_1\omega)^2.
\end{aligned}
\tag{4.5}
$$

Using MATLAB to simplify the above equation, we get:

$$
\Rightarrow \omega^{14} + u_1\omega^{12} + u_2\omega^{10} + u_3\omega^8 + u_4\omega^6 + u_5\omega^4 + u_6\omega^2 + u_7 = 0, \tag{4.6}
$$

where,

$$
\begin{aligned}
u_1 &= -2p_5 + {p_6}^2 - {q_6}^2,\\
u_2 &= 2p_3 - 2p_4p_6 + {p_5}^2 + 2q_4q_6 - {q_5}^2,\\
u_3 &= -2p_1 + 2p_2p_6 - 2p_3p_5 + {p_4}^2 - 2q_2q_6 + 2q_3q_5 - {q_4}^2,\\
u_4 &= -2p_0p_6 + 2p_1p_5 - 2p_2p_4 + {p_3}^2 + 2q_0q_6 - 2q_1q_5 + 2q_2q_4 - {q_3}^2,\\
u_5 &= 2p_0p_4 - 2p_1p_3 + {p_2}^2 - 2q_0q_4 + 2q_1q_3 - {q_2}^2,\\
u_6 &= -2p_0p_2 + {p_1}^2 + 2q_0q_2 - {q_1}^2,\\
u_7 &= {p_0}^2 - {q_0}^2.
\end{aligned}
\tag{4.7}
$$

Put, $s = \omega^2$ in Eq. (4.6), then we have:

$$
s^7 + u_1s^6 + u_2s^5 + u_3s^4 + u_4s^3 + u_5s^2 + u_6s^1 + u_7 = 0. \tag{4.8}
$$

If we assume $|H_n| > 0$ for $n = 1, \ldots, 7$, where for each n, H_n is a Hurwitz matrix of order $n * n$, with general form:

$$
H_n = \begin{bmatrix}
u_1 & 1 & 0 & 0 & \ldots & 0\\
u_3 & u_2 & u_1 & 1 & \ldots & 0\\
u_5 & u_4 & u_3 & u_2 & \ldots & 0\\
\vdots & \vdots & \vdots & \vdots & \ddots & \vdots\\
0 & 0 & 0 & 0 & 0 & u_n
\end{bmatrix}, \tag{4.9}
$$

with $u_j = 0$ if $j > 7$ or $j < 0$.

Then by Routh–Hurwitz criterion the roots of Eq. (4.8) will have negative real parts. However, there does not exist ω such that $s = \omega^2$ is negative. This poses a contradiction. Therefore, the conditions in (4.9) are sufficient to conclude that all the roots of Eq. (4.3) for $\tau > 0$ have negative real parts. Hence, we have the following theorem.

Theorem 5. *Let E_1 be an endemic equilibrium point of system (2.2). Then for $\tau \geq 0$, E_1 is locally asymptotically stable if for each of the seven Hurwitz matrices defined as in (4.9), $|H_n| > 0$ and for each of the seven Hurwitz matrices defined as in (3.17), $|H_n'| > 0$.*

4.3.1. Hopf bifurcation of endemic equilibrium point

In the previous subsection, we listed conditions for local stability of E_1 for $\tau > 0$. However, if these conditions are not satisfied, then E_1 looses its stability. In this subsection, we will work to obtain the conditions for local stability of E_1 based on the delay parameter and will determine the critical value of τ (i.e., τ_0), post which E_1 ceases to be locally stable.

Consider that $|H_n| < 0$ for at least one of the seven Hurwitz matrices defined in (4.9). Then, there will be at least one root of Eq. (4.3), that will not have negative real part. Also, in order for Eq. (4.3) to have a root with positive real part, Eq. (4.3) must have a purely imaginary root. Further, this is possible only when Eq. (4.8) has a positive real root. Let Eq. (4.8) be rewritten as:

$$f(s) = s^7 + u_1 s^6 + u_2 s^5 + u_3 s^4 + u_4 s^3 + u_5 s^2 + u_6 s^1 + u_7 = 0.$$

It can be seen that, $f(0) = u_7$ and $\lim_{s\to\infty} f(s) = \infty$. Then, $f(s) = 0$ will have a positive real root only if $u_7 < 0$. Now, let $\lambda(\tau) = \eta(\tau) + \iota\omega(\tau)$ with $\omega > 0$ be the root of (4.3) such that for a particular $\tau_0 > 0$, we have, $\eta(\tau_0) = 0$ and $\omega(\tau_0) = \omega_0$, so that, $\lambda = \iota\omega_0$ is a purely imaginary root of (4.3). Then, for $\tau < \tau_0$ we have $\eta(\tau) < 0$ and E_1 is stable; for $\tau > \tau_0$ we have $\eta(\tau) > 0$ and E_1 is unstable; and for $\tau = \tau_0$ we have $\eta(\tau_0) = 0$ and E_1 undergoes Hopf bifurcation at τ_0. We can obtain the critical value of τ (for $n = 0, 1, 2, \ldots$) from Eq. (4.4) by replacing $\omega = \omega_0$ and solving for the variables $\sin\omega_0\tau_0$ and $\cos\omega_0\tau_0$:

$$\tau_n = \frac{\arcsin\left(\frac{(p_6\omega_0^6 - p_4\omega_0^4 + p_2\omega_0^2 - p_0)(q_5\omega_0^5 - q_3\omega_0^3 + q_1\omega_0) + (\omega_0^7 - p_5\omega_0^5 + p_3\omega_0^3 - p_1\omega_0)(q_6\omega_0^6 - q_4\omega_0^4 + q_2\omega_0^2 - q_0)}{(q_5\omega_0^5 - q_3\omega_0^3 + q_1\omega_0)^2 + (q_6\omega_0^6 - q_4\omega_0^4 + q_2\omega_0^2 - q_0)^2}\right)}{\omega_0} + \frac{2\pi n}{\omega_0},$$

where, $\tau_0 = min\{\tau_n : n = 0, 1, 2, \ldots\}$.

Next, for the existence of the Hopf bifurcation, we prove that the following transversality condition is satisfied:

$$\frac{d}{d\tau}(Re(\lambda))\bigg|_{\tau=\tau^*} = \frac{d}{d\tau}(Re(\lambda))\bigg|_{\lambda=\iota\omega_0} > 0. \tag{4.10}$$

Differentiating (4.3) with τ, we get:

$$\begin{aligned}
&(7\lambda^6 + 6p_6\lambda^5 + 5p_5\lambda^4 + 4p_4\lambda^3 + 3p_3\lambda^2 + 2p_2\lambda + p_1)\frac{d\lambda}{d\tau} \\
&+ e^{-\lambda\tau}(6q_6\lambda^5 + 5q_5\lambda^4 + 4q_4\lambda^3 + 3q_3\lambda^2 + 2q_2\lambda + q_1)\frac{d\lambda}{d\tau} \\
&+ (q_6\lambda^6 + q_5\lambda^5 + q_4\lambda^4 + q_3\lambda^3 + q_2\lambda^2 + q_1\lambda + q_0)e^{-\lambda\tau}(-\lambda - \tau\frac{d\lambda}{d\tau}) = 0, \\
&\Rightarrow \begin{bmatrix} (7\lambda^6 + 6p_6\lambda^5 + 5p_5\lambda^4 + 4p_4\lambda^3 + 3p_3\lambda^2 + 2p_2\lambda + p_1) \\ +e^{-\lambda\tau}(6q_6\lambda^5 + 5q_5\lambda^4 + 4q_4\lambda^3 + 3q_3\lambda^2 + 2q_2\lambda + q_1) \\ -\tau e^{-\lambda\tau}(q_6\lambda^6 + q_5\lambda^5 + q_4\lambda^4 + q_3\lambda^3 + q_2\lambda^2 + q_1\lambda + q_0) \end{bmatrix}\left(\frac{d\lambda}{d\tau}\right) \\
&= \lambda e^{-\lambda\tau}(q_6\lambda^6 + q_5\lambda^5 + q_4\lambda^4 + q_3\lambda^3 + q_2\lambda^2 + q_1\lambda + q_0), \\
&\Rightarrow \left(\frac{d\lambda}{d\tau}\right)^{-1} = \frac{\begin{bmatrix} (7\lambda^6 + 6p_6\lambda^5 + 5p_5\lambda^4 + 4p_4\lambda^3 + 3p_3\lambda^2 + 2p_2\lambda + p_1) \\ +e^{-\lambda\tau}(6q_6\lambda^5 + 5q_5\lambda^4 + 4q_4\lambda^3 + 3q_3\lambda^2 + 2q_2\lambda + q_1) \\ -\tau e^{-\lambda\tau}(q_6\lambda^6 + q_5\lambda^5 + q_4\lambda^4 + q_3\lambda^3 + q_2\lambda^2 + q_1\lambda + q_0) \end{bmatrix}}{\lambda e^{-\lambda\tau}(q_6\lambda^6 + q_5\lambda^5 + q_4\lambda^4 + q_3\lambda^3 + q_2\lambda^2 + q_1\lambda + q_0)}, \\
&\Rightarrow \left(\frac{d\lambda}{d\tau}\right)^{-1} = \begin{bmatrix} \frac{(7\lambda^6 + 6p_6\lambda^5 + 5p_5\lambda^4 + 4p_4\lambda^3 + 3p_3\lambda^2 + 2p_2\lambda + p_1)}{\lambda e^{-\lambda\tau}(q_6\lambda^6 + q_5\lambda^5 + q_4\lambda^4 + q_3\lambda^3 + q_2\lambda^2 + q_1\lambda + q_0)} \\ +\frac{(6q_6\lambda^5 + 5q_5\lambda^4 + 4q_4\lambda^3 + 3q_3\lambda^2 + 2q_2\lambda + q_1)}{\lambda(q_6\lambda^6 + q_5\lambda^5 + q_4\lambda^4 + q_3\lambda^3 + q_2\lambda^2 + q_1\lambda + q_0)} \\ -\frac{\tau}{\lambda} \end{bmatrix}, \\
&\Rightarrow \left(\frac{d\lambda}{d\tau}\right)^{-1} = \begin{bmatrix} \frac{(7\lambda^6 + 6p_6\lambda^5 + 5p_5\lambda^4 + 4p_4\lambda^3 + 3p_3\lambda^2 + 2p_2\lambda + p_1)}{-\lambda(\lambda^7 + p_6\lambda^6 + p_5\lambda^5 + p_4\lambda^4 + p_3\lambda^3 + p_2\lambda^2 + p_1\lambda + p_0)} \\ +\frac{(6q_6\lambda^5 + 5q_5\lambda^4 + 4q_4\lambda^3 + 3q_3\lambda^2 + 2q_2\lambda + q_1)}{\lambda(q_6\lambda^6 + q_5\lambda^5 + q_4\lambda^4 + q_3\lambda^3 + q_2\lambda^2 + q_1\lambda + q_0)} \\ -\frac{\tau}{\lambda} \end{bmatrix},
\end{aligned}$$

where, we have substituted the relation from Eq. (4.3):

$$-(\lambda^7 + p_6\lambda^6 + p_5\lambda^5 + p_4\lambda^4 + p_3\lambda^3 + p_2\lambda^2 + p_1\lambda + p_0) = e^{-\lambda\tau}(q_6\lambda^6 + q_5\lambda^5 + q_4\lambda^4 + q_3\lambda^3 + q_2\lambda^2 + q_1\lambda + q_0).$$

Now,

$$\frac{d}{d\tau}(Re(\lambda))^{-1}\Big|_{\lambda=\iota\omega_0}$$
$$= Re\left(\frac{d\lambda}{d\tau}\right)^{-1}\Big|_{\lambda=\iota\omega_0},$$
$$= Re\left(\begin{array}{c}\dfrac{(-7\omega_0^6+\iota 6p_6\omega_0^5+5p_5\omega_0^4+-\iota 4p_4\omega_0^3-3p_3\omega_0^2+\iota 2p_2\omega_0+p_1)}{-\iota\omega_0(-\iota\omega_0^7-p_6\omega_0^6+\iota p_5\omega_0^5+p_4\omega_0^4-\iota p_3\omega_0^3-p_2\omega_0^2+\iota p_1\omega_0-p_0)}\\ +\dfrac{(\iota 6q_6\omega_0^5+5q_5\omega_0^4-\iota 4q_4\omega_0^3-3q_3\omega_0^2+\iota 2q_2\omega_0+q_1)}{\iota\omega_0(-q_6\omega_0^6+\iota q_5\omega_0^5+q_4\omega_0^4-\iota q_3\omega_0^3-q_2\omega_0^2+\iota q_1\omega_0+q_0)}\\ -\dfrac{\tau}{\iota\omega_0}\end{array}\right),$$
$$= \frac{1}{\omega_0}Re\left(\begin{array}{c}\dfrac{(-7\omega_0^6+5p_5\omega_0^4-3p_3\omega_0^2+p_1)+\iota(6p_6\omega_0^5-4p_4\omega_0^3+2p_2\omega_0)}{(-\omega_0^7+p_5\omega_0^5-p_3\omega_0^3+p_1\omega_0)+\iota(p_6\omega_0^6-p_4\omega_0^4+p_2\omega_0^2-p_0)}\\ +\dfrac{(5q_5\omega_0^4-3q_3\omega_0^2+q_1)+\iota(6q_6\omega_0^5-4q_4\omega_0^3+2q_2\omega_0)}{(-q_5\omega_0^5+q_3\omega_0^3-q_1\omega_0)+\iota(-q_6\omega_0^6+q_4\omega_0^4-q_2\omega_0^2+q_0)}\\ -\dfrac{\tau}{\iota}\end{array}\right),$$

Rationalizing the first two terms above, we get the expression:

$$= \frac{1}{\omega_0}\left(\begin{array}{c}\dfrac{(-7\omega_0^6+5p_5\omega_0^4-3p_3\omega_0^2+p_1)(-\omega_0^7+p_5\omega_0^5-p_3\omega_0^3+p_1\omega_0)+(6p_6\omega_0^5-4p_4\omega_0^3+2p_2\omega_0)(p_6\omega_0^6-p_4\omega_0^4+p_2\omega_0^2-p_0)}{(-\omega_0^7+p_5\omega_0^5-p_3\omega_0^3+p_1\omega_0)^2+(p_6\omega_0^6-p_4\omega_0^4+p_2\omega_0^2-p_0)^2}\\ +\dfrac{(5q_5\omega_0^4-3q_3\omega_0^2+q_1)(-q_5\omega_0^5+q_3\omega_0^3-q_1\omega_0)+(6q_6\omega_0^5-4q_4\omega_0^3+2q_2\omega_0)(-q_6\omega_0^6+q_4\omega_0^4-q_2\omega_0^2+q_0)}{(-q_5\omega_0^5+q_3\omega_0^3-q_1\omega_0)^2+(-q_6\omega_0^6+q_4\omega_0^4-q_2\omega_0^2+q_0)^2}\end{array}\right).$$

Using Eq. (4.5) we know the two denominators are equal to each other. Also cancelling out w_0 we get:

$$= \frac{\left(\begin{array}{c}(-7\omega_0^6+5p_5\omega_0^4-3p_3\omega_0^2+p_1)(-\omega_0^6+p_5\omega_0^4-p_3\omega_0^2+p_1)\\ +(6p_6\omega_0^4-4p_4\omega_0^2+2p_2)(p_6\omega_0^6-p_4\omega_0^4+p_2\omega_0^2-p_0)\\ +(5q_5\omega_0^4-3q_3\omega_0^2+q_1)(-q_5\omega_0^4+q_3\omega_0^2-q_1)\\ +(6q_6\omega_0^4-4q_4\omega_0^2+2q_2)(-q_6\omega_0^6+q_4\omega_0^4-q_2\omega_0^2+q_0)\end{array}\right)}{(-\omega_0^7+p_5\omega_0^5-p_3\omega_0^3+p_1\omega_0)^2+(p_6\omega_0^6-p_4\omega_0^4+p_2\omega_0^2-p_0)^2}.$$

Using MATLAB to solve the numerator, we get:

$$= \frac{\left(\begin{array}{c}7\omega_0^{12}+6(-2p_5+{p_6}^2-{q_6}^2)\omega_0^{10}+5(2p_3-2p_4p_6+{p_5}^2+2q_4q_6-{q_5}^2)\omega_0^8\\ +4(-2p_1+2p_2p_6-2p_3p_5+{p_4}^2-2q_2q_6+2q_3q_5-{q_4}^2)\omega_0^6\\ +3(-2p_0p_6+2p_1p_5-2p_2p_4+{p_3}^2+2q_0q_6-2q_1q_5+2q_2q_4-{q_3}^2)\omega_0^4\\ +2(2p_0p_4-2p_1p_3+{p_2}^2-2q_0q_4+2q_1q_3-{q_2}^2)\omega_0^2\\ +(-2p_0p_2+{p_1}^2+2q_0q_2-{q_1}^2)\end{array}\right)}{(-\omega_0^7+p_5\omega_0^5-p_3\omega_0^3+p_1\omega_0)^2+(p_6\omega_0^6-p_4\omega_0^4+p_2\omega_0^2-p_0)^2}.$$

Substituting from Eq. (4.7), we get:

$$= \frac{7\omega_0^{12}+6u_1\omega_0^{10}+5u_2\omega_0^8+4u_3\omega_0^6+3u_4\omega_0^4+2u_5\omega_0^2+u_6}{(-\omega_0^7+p_5\omega_0^5-p_3\omega_0^3+p_1\omega_0)^2+(p_6\omega_0^6-p_4\omega_0^4+p_2\omega_0^2-p_0)^2}.$$

Clearly, in the above equation denominator is positive. Also, if $u_1, u_2, \ldots, u_7 > 0$ then numerator is positive. Hence, $\frac{d}{d\tau}(Re(\lambda))^{-1}\Big|_{\lambda=\iota\omega_0} > 0$ if $u_1, u_2, \ldots, u_6 > 0$.

We summarize the above discussion in the following theorem.

Theorem 6. *Let E_1 be an endemic equilibrium point of system (2.2) satisfying all the conditions in (3.17).*

1. *If all the Hurwitz matrices defined in (4.9) are such that $|H_n| > 0$, then E_1 is locally asymptotically stable for all $\tau \geq 0$.*

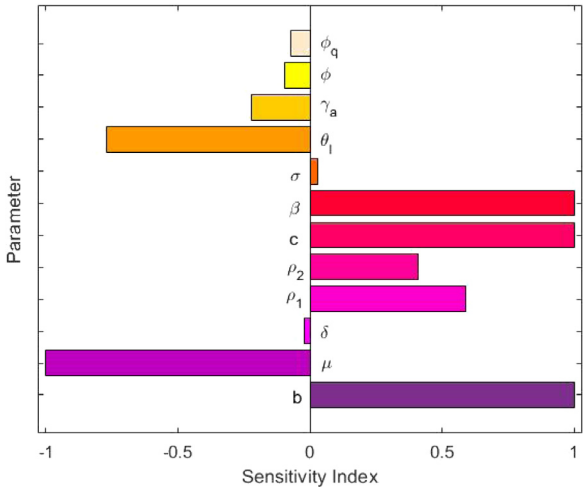

Fig. 2. Sensitivity Index of R_0 in response to change in different parameters.

2. *If at least one of the Hurwitz matrices defined in (4.9) is such that* $|H_n| < 0$ *and* $u_7 < 0$*, then* E_1 *is locally asymptotically stable for* $\tau \in [0, \tau_0)$ *and* E_1 *is unstable for* $\tau > \tau_0$.
3. *If at least one of the Hurwitz matrices defined in (4.9) is such that* $|H_n| < 0$*,* $u_7 < 0$ *and the transversality condition in (4.10) holds true, then the system undergoes a Hopf bifurcation at* E_1 *when* $\tau = \tau_0$.

Remark: Choosing τ as the hopf bifurcation parameter helps us understand the dependence of epidemic transmission on the delay (over and above the mean incubation period) in development of symptoms in infected individuals. Theorem 6 suggests that an infectious disease can be easily controlled and the system is asymptotically stable if τ is under a certain critical level, but the level of infection in the system undergoes fluctuations once the delay reaches the critical level. From a biological point of view these fluctuations can be viewed as the frequent ups and downs in the cases during an epidemic. For instance, during current COVID-19 crisis the number of infected individuals kept on fluctuating. There were times when the disease seemed to be under control but it was followed by a sudden increase of infected individuals. This is an example of hopf bifurcation. Although controlling the development of symptoms is practically out of our hands, but being aware of the critical value of the delay can help us proactively deal with the fluctuating stability, for instance, large scale testings can be prioritized in order to identify infected individuals and provide necessary treatment or isolate them so as to prevent further infection.

In the next subsection, we have discussed sensitivity of R_0 to various parameters.

4.4. Sensitivity of basic reproduction number(R_0)

R_0 is an important tools in epidemiological modelling. In Section 3.2, we have already derived a formula for R_0 using the next generation matrix method. In this section, we calculate the sensitivity index of R_0 in response to various parameters of the model. In plain words, sensitivity index is a measure of how much R_0 changes with respect to a changing parameter. In order to compute the sensitivity index of R_0 in response to a parameter Y, we use the following formula [80]:

$$\varphi_{R_0}{}^{Y} = \frac{\partial R}{\partial Y}\frac{Y}{R_0}.$$

The sensitivity index of R_0 corresponding to different parameters has been listed in Table 2 and shown graphically in Fig. 2. It is to be noted that Table 2 lists an index only for those parameters that appear in the formula for R_0 (see Eq. (3.2)), for all other parameters there is no direct dependence of R_0 on them.

The sign of the indices refers to the nature of change (increase/decrease) in R_0 in response to the changing parameters while the value of the indices refers to the magnitude of this change. For instance, in the bar graph in Fig. 2, for every parameter having a bar pointing in the right direction, there will be an increase in R_0 when the parameter increases while for all those with bars lying towards the left, R_0 decreases as these increase. Further, it can be seen from Table 2 that $\varphi_{R_0}{}^{\beta} = +1.000$), meaning that R_0 will increase by 1% when β increases by 1%. Similarly, $\varphi_{R_0}{}^{\theta_I} = -0.7689$, means that R_0 will decrease by 0.7689% when θ_I increases by 1%.

It can also be observed that R_0 has the strongest negative relation with μ while it has a strongest positive relation with b, β and c. Further, Figs. 3(a) and 3(b) show contour plots of R_0 as a function of two parameters μ, β and β, c, respectively. From Fig. 3(a) it is clear that R_0 increases with the increasing β and decreasing μ. Similarly, Fig. 3(b) shows how R_0 increases with increase in β and c. Since, R_0 has a direct impact on the spread of the disease, it is important to be aware of its dependence on different parameters, to be able to take appropriate steps to decrease it. For instance, since the COVID-19 pandemic have started, countries all over the

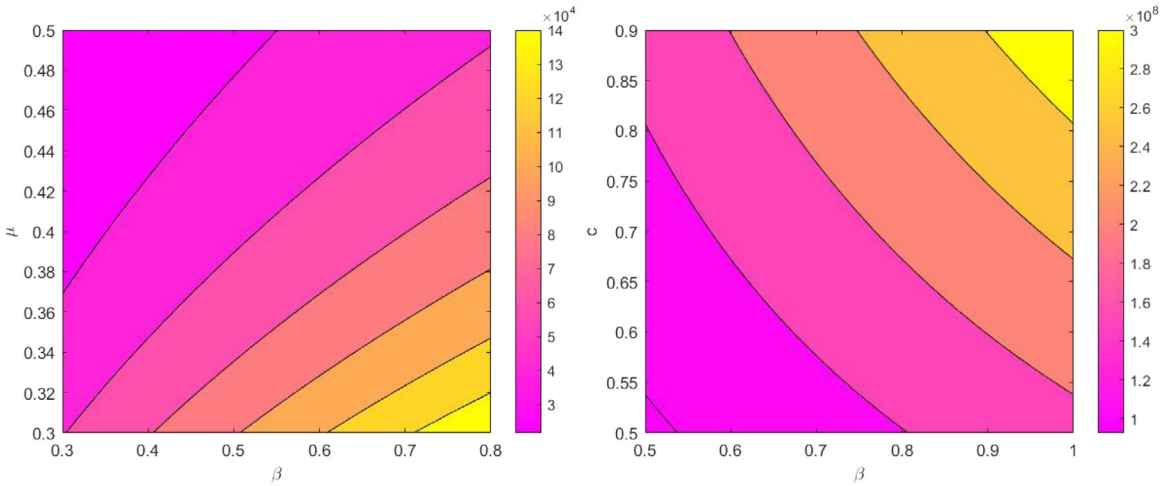

(a) R_0 in terms of β and μ (b) R_0 in terms of β and c

Fig. 3. Contour plot of R_0 as a function of only two variables.

Table 2
Values of parameters and the sensitivity indices.

Parameter	Value	Index
b	52,098	1.00000
μ	$3.63 * 10^{-5}$	−1.0002
δ	0.0001 day^{-1}	−0.0001
ρ_1	0.15	0.5899
ρ_2	0.1	0.4101
ρ_3	0.2	NA
α	$1 * 10^{-15}$	NA
c	14.781	1.0000
β	$5.62 * 10^{-10}$	1.0000
σ	0.19 day^{-1}	0.0002
θ_I	0.98 day^{-1}	−0.7689
γ	0.07 day^{-1}	NA
γ_a	0.9 day^{-1}	−0.2211
γ_q	0.9 day^{-1}	NA
ϕ	0.76 day^{-1}	−0.0076
ϕ_q	0.009 day^{-1}	−0.0022
$\triangle$	0.00025	NA

world have been focusing on social distancing and imposing lockdown, which now makes sense because this way they have been able to bring down the parameters like β and c which correspond to the probability of transmission per contact and contact rate, respectively. However, it is important to note that controlling certain parameters is out of our hands and no meddling can be done with these to decrease R_0, but a mere knowledge about the dependence can help us take proactive decisions.

In the next section, we introduce various control strategies and try to look for optimal control, so that suitable policies can be implemented for controlling the disease.

5. Optimal control problem

In this section, we aim to reduce infection in system using various controllers. Our aim is to see fewer people become sick and more people recover from infection. In our proposed model we introduce four control variables u_1, u_2, u_3 u_4. The first control variable $u_1(t)$ is applied on the recruitment of susceptible individuals. It is assumed that the 'Susceptible' class has a constant recruitment rate of $(1-u_1(t))bN$ and individuals self-isolate themselves at a rate of $u_1(t)bN$ and move directly to the 'Recovered/Removed' class. The second control variable $u_2(t)$, is applied on the contact rate c and refers to the preventive measures (like social distancing, using mask, sanitizing, etc.) that can be taken by the susceptible class to avoid getting exposed/infected. As assumed in the proposed model, the symptomatic individuals move to the hospitalized compartment and receive treatment. However, due to several reasons (like, financial bounds or lack of information or misinformation) a lot of symptomatic individuals resist from getting hospitalized. Therefore, $u_3(t)$ is applied on the 'Symptomatic' class and refers to the government initiative of tracking and hospitalizing more and more individuals showing symptoms. The model proposes that 'Quarantined' individuals show mild symptoms and can recover

naturally while under home isolation. However, certain individuals may exhibit severe symptoms and may require medical help. Therefore, the fourth control variable $u_4(t)$, is applied on the 'Quarantined' class and refers to the frequent monitoring of quarantined individuals by government in order to hospitalize the one's that need medical care. A real-life application of $u_3(t)$ and $u_4(t)$ is how government kept a data base of all infected individuals and also reached them on regular basis via calls, in order to keep a check on their condition.

Let, $[0, t_{end}]$ be the time interval over which the control strategies are applied in the system. Then relative to the seven state variables $(S(t), E(t), I(t), I_a(t), I_q(t), H(t), R(t))$, the admissible set of control variables is defined as:

$$U = \{(u_1(t), u_2(t), u_3(t), u_4(t)) : \ 0 \le u_i(t) \le 1 \text{ is Lebesgue integrable; for } i = 1,2,3,4 \text{ and } t \in [0, t_{end}]\}. \tag{5.1}$$

Introducing the control variables $u_1(t), u_2(t), u_3(t), u_4(t)$ in system (2.2), we obtain the control system for the optimal control problem as follows:

$$\begin{cases} \frac{dS}{dt} = b(1-u_1(t)) - \beta c(1-u_2(t))SI_a - \frac{\beta c(1-u_2(t))SI}{1+\alpha I} - \mu S + \triangle R, \\ \frac{dE}{dt} = \beta c(1-u_2(t))SI_a + \frac{\beta c(1-u_2(t))SI}{1+\alpha I} - (\sigma+\mu)E, \\ \frac{dI}{dt} = \rho_1\sigma E + \phi I_a(t-\tau) - (\theta_I + \mu + \delta)I - u_3(t)I, \\ \frac{dI_a}{dt} = \rho_2\sigma E - (\phi_q + \gamma_a + \mu)I_a - \phi I_a(t-\tau), \\ \frac{dI_q}{dt} = \rho_3\sigma E + \phi_q I_a - (\gamma_q + \mu + \delta)I_q - u_4(t)I_q, \\ \frac{dH}{dt} = \theta_I I - (\gamma + \mu + \delta)H + u_3(t)I + u_4(t)I_q, \\ \frac{dR}{dt} = \gamma_a I_a + \gamma_q I_q + \gamma H - (\triangle + \mu)R + bu_1(t), \end{cases} \tag{5.2}$$

with initial conditions,

$$S(0) = S_0,\ E(0) = E_0,\ I(0) = I_0,\ I_a(0) = I_{a0},\ I_q(0) = I_{q0},\ H(0) = H_0, \text{ and } R(0) = R_0. \tag{5.3}$$

Before formulating the optimal control problem, it is important to show the existence of solution of control system (5.2).

5.1. Existence of solution of the control system

In order to show the existence of solution of the control system (5.2), we represent the control system (5.2) as follows:

$$\frac{dV(t)}{dt} = AV(t) + F(V(t), V_\tau(t)) + C(u, V(t)), \tag{5.4}$$

where,

$$V(t) = \begin{bmatrix} S(t) \\ E(t) \\ I(t) \\ I_a(t) \\ I_q(t) \\ H(t) \\ R(t) \end{bmatrix}, A = \begin{bmatrix} -\mu & 0 & 0 & 0 & 0 & 0 & \triangle \\ 0 & -\sigma-\mu & 0 & 0 & 0 & 0 & 0 \\ 0 & \rho_1\sigma & -\mu-\delta-\theta_I & 0 & 0 & 0 & 0 \\ 0 & \rho_2\sigma & 0 & -\phi_q-\gamma_a-\mu & 0 & 0 & 0 \\ 0 & \rho_3\sigma & 0 & \phi_q & -\gamma_q-\delta-\mu & 0 & 0 \\ 0 & 0 & \theta_I & 0 & 0 & -\gamma-\delta-\mu & 0 \\ 0 & 0 & 0 & \gamma_a & \gamma_q & \gamma & -\triangle-\mu \end{bmatrix},$$

$$F(V(t), V_\tau(t)) = \begin{bmatrix} -\beta c S I_a - \frac{\beta c S I}{1+\alpha I} \\ \beta c S I_a + \frac{\beta c S I}{1+\alpha I} \\ \phi I_a(t-\tau) \\ -\phi I_a(t-\tau) \\ 0 \\ 0 \\ 0 \end{bmatrix}, C(u, V(t)) = \begin{bmatrix} b(1-u_1(t)) + \beta c u_2(t) S I_a + \frac{\beta c u_2(t) S I}{1+\alpha I} \\ -u_2(t)\beta c S I_a - \frac{\beta c u_2(t) S I}{1+\alpha I} \\ -u_3(t) I \\ 0 \\ -u_4(t) I_q \\ u_3(t) I + u_4(t) I_q \\ b u_1(t) \end{bmatrix},$$

and, $V_\tau(t) = V(t-\tau)$. The system (5.4) is a non-linear system with a bounded coefficient. Set,

$$G(V(t), V_\tau(t)) = AV(t) + F(V(t), V_\tau(t)). \tag{5.5}$$

We have,

$$F(V_1(t),(V_1)_\tau(t)) - F(V_2(t),(V_2)_\tau(t)) = \begin{bmatrix} -\left(\beta c S_1 I_{a1} + \frac{\beta c S_1 I_1}{1+\alpha I_1} + \beta c S_2 I_{a2} + \frac{\beta c S_2 I_2}{1+\alpha I_2}\right) \\ \beta c S_1 I_{a1} + \frac{\beta c S_1 I_1}{1+\alpha I_1} + \beta c S_2 I_{a2} + \frac{\beta c S_2 I_2}{1+\alpha I_2} \\ \phi(I_{a1})_\tau - \phi(I_{a2})_\tau \\ -(\phi(I_{a1})_\tau - \phi(I_{a2})_\tau) \\ 0 \\ 0 \\ 0 \end{bmatrix},$$

where, $(I_{ai})_\tau = I_{ai}(t-\tau)$ for $i = 1, 2$.

Now, the second term on the right hand side of Eq. (5.5) satisfies:

$$\begin{aligned}
&|F(V_1(t),(V_1)_\tau(t)) - F(V_2(t),(V_2)_\tau(t))| \\
&\quad = \left|-\left(\beta c S_1 I_{a1} + \frac{\beta c S_1 I_1}{1+\alpha I_1} + \beta c S_2 I_{a2} + \frac{\beta c S_2 I_2}{1+\alpha I_2}\right)\right| + \left|\beta c S_1 I_{a1} + \frac{\beta c S_1 I_1}{1+\alpha I_1} + \beta c S_2 I_{a2} + \frac{\beta c S_2 I_2}{1+\alpha I_2}\right| \\
&\qquad + |\phi(I_{a1})_\tau - \phi(I_{a2})_\tau| + |-(\phi(I_{a1})_\tau - \phi(I_{a2})_\tau)|, \\
&\quad \le 2\beta c\left|S_1 I_{a1} + \frac{S_1 I_1}{1+\alpha I_1} - S_2 I_{a2} - \frac{S_2 I_2}{1+\alpha I_2}\right| + 2\phi|(I_{a1})_\tau - (I_{a2})_\tau|, \\
&\quad \le 2\beta c\left|S_1 I_{a1}(1+\alpha I_1)(1+\alpha I_2) + S_1 I_1(1+\alpha I_2) - S_2 I_{a2}(1+\alpha I_1)(1+\alpha I_2) - S_2 I_2(1+\alpha I_1)\right| \\
&\qquad + 2\phi|(I_{a1})_\tau - (I_{a2})_\tau|, \\
&\quad = 2\beta c\Big|I_{a1}(S_1 - S_2) + S_2(I_{a1} - I_{a2}) + \alpha S_1 I_1(I_{a1} - I_{a2}) + \alpha I_1 I_{a2}(S_1 - S_2) + \alpha I_2 I_{a1}(S_1 - S_2) \\
&\qquad + \alpha S_2 I_2(I_{a1} - I_{a2}) + \alpha^2 S_1 I_1 I_2(I_{a1} - I_{a2}) + \alpha^2 I_1 I_2 I_{a2}(S_1 - S_2) + S_1(I_1 - I_2) + I_2(S_1 - S_2) \\
&\qquad + \alpha I_1 I_2(S_1 - S_2)\Big| + 2\phi|(I_{a1})_\tau - (I_{a2})_\tau|, \\
&\quad \le 2\beta c(|I_2| + |I_{a1}| + \alpha|I_1\|I_2| + \alpha|I_1\|I_{a2}| + \alpha|I_2\|I_{a1}| + \alpha^2|I_1\|I_2\|I_{a2}|)|S_1 - S_2| + 2\beta c|S_1\|I_1 - I_2| \\
&\qquad + 2\beta c(|S_2| + \alpha|S_1\|I_1| + \alpha|S_2\|I_2| + \alpha^2|S_1\|I_1\|I_2|)|I_{a1} - I_{a2}| + 2\phi|I_{a1}(t-\tau) - I_{a2}(t-\tau)|, \\
&\quad \le M_1(|S_1 - S_2| + |I_1 - I_2| + |I_{a1} - I_{a2}|) + M_2|I_{a1}(t-\tau) - I_{a2}(t-\tau)|, \\
&\quad \le M_1|V_1(t) - V_2(t)| + M_2|(V_1)_\tau(t) - (V_2)_\tau(t)|,
\end{aligned}$$

where, M_1 and M_2 are positive constants as defined below and are independent of S, E, I, I_a, I_q, H and R:

$$M_1 = max\left(\frac{2\beta bc}{\mu}\left(2 + 3\alpha\frac{b}{\mu} + \alpha^2\frac{b^2}{\mu^2}\right); \frac{2\beta bc}{\mu}; \frac{2\beta bc}{\mu}\left(1 + 2\alpha\frac{b}{\mu} + \alpha^2\frac{b^2}{\mu^2}\right)\right), \text{ and}$$

$$M_2 = 2\phi.$$

Then, it can be easily shown that: $|G(V_1, V_{1\tau}) - G(V_2, V_{2\tau})| \le L(|V_1(t) - V_2(t)| + |(V_1)_\tau(t) - (V_2)_\tau(t)|)$

Here, $L = \max\{M_1, M_2, \|A\|\} < \infty$. Thus, it follows that the function G is uniformly Lipschitz continuous. As done by Zaman et al. [81], using the definition of U and the non-negativity restriction on the state variables, we conclude that a solution of control system (5.2) exists.

5.2. Formulation of the optimal control problem

Now, we formulate the optimal control problem. The objective functional is,

$$J(u_1, u_2, u_3, u_4) = \int_0^{t_{end}} (A_1 E + A_2 I + A_3 I_a + \epsilon_1 {u_1}^2 + \epsilon_2 {u_2}^2 + \epsilon_3 {u_3}^2 + \epsilon_4 {u_4}^2)\, dt, \tag{5.6}$$

subject to, the control system (5.2) and initial conditions stated in (5.3).

Our aim is to minimize the cost functional (5.6), which involves minimizing the populations, Exposed (E), Symptomatic (I) and Asymptomatic (I_a) along with minimizing the socio-economic costs associated with resources required for self isolation given by ϵu_1^2, social distancing measures, sanitizing methods, using masks, and etc given by ϵu_2^2, tracking and testing of symptomatic individuals given by ϵu_3^2 and tracing Quarantined individuals requiring medical help given by ϵu_4^2. Here, A_i (for $i = 1, 2, 3$) and ϵ_j (for $j = 1, 2, 3, 4$) are the weight constants and denotes the relative cost of interventions over $[0, t_{end}]$. Therefore, we want to find an optimal control pair $(u_1^*, u_2^*, u_3^*, u_4^*)$ such that the objective functional in (5.6) is minimized.

In the two subsections that follow, we show the existence of the optimal control pair followed by finding the Lagrangian and Hamiltonian of the control problem, and then using the Pontryagin's Maximum Principle to obtain the optimal control pair.

5.3. Existence of optimal control pair

Theorem 7. *There exists an optimal control pair* $(u_1{}^*, u_2{}^*, u_3{}^*, u_4{}^*)$ *such that*

$$J(u_1{}^*, u_2{}^*, u_3{}^*, u_4{}^*) = min\{J(u_1, u_2, u_3, u_4) : (u_1, u_2, u_3, u_4,) \in U\}$$

subject to the control system (5.2) *and the initial conditions* (5.3).

Proof. We prove the existence of the optimal control pair using a result by Lukes [82]. Consider the following properties of the optimal control problem given by (5.2), (5.3) and (5.6):

1. The control variables u_1, u_2, u_3 and u_4 along with the state variables $S(t)$, $E(t)$, $I(t)$, $I_a(t)$, $I_q(t)$, $H(t)$ and $R(t)$ are nonempty by definition.
2. The admissible set of control variables U, is closed and convex by definition.
3. The optimal system is bounded which determines the compactness required for the existence of the optimal control.
4. The integrand of the objective functional is convex on the admissible set of control variables U.
5. There exists constants $\omega_1, \omega_2 > 0$ and $\rho > 1$ such that the integrand of the objective functional $(A_1E + A_2I + A_3I_a + \epsilon_1{u_1}^2 + \epsilon_2{u_2}^2 + \epsilon_3{u_3}^2 + \epsilon_4{u_4}^2)$ satisfies,

$$A_1E + A_2I + A_3I_a + \epsilon_1{u_1}^2 + \epsilon_2{u_2}^2 + \epsilon_3{u_3}^2 + \epsilon_4{u_4}^2 \geq \omega_1 + \omega_2(|u_1|^2 + |u_2|^2 + |u_3|^2 + |u_4|^2)^{\frac{\rho}{2}}.$$

As done by Abta et al. [83], the existence of the optimal control pair can now be proved using the result by Lukes [82]. □

5.4. Characterization of optimal control pair

The Lagrangian of the optimal control problem is:

$$L(E, I, I_a, u_1, u_2, u_3, u_4) = A_1E(t) + A_2I(t) + A_3I_a(t) + \epsilon_1{u_1}^2(t) + \epsilon_2{u_2}^2(t) + \epsilon_3{u_3}^2(t) + \epsilon_4{u_4}^2(t).$$

Consider,

$$X(t) = (S(t), E(t), I(t), I_a(t), I_q(t), H(t), R(t)) \text{and}$$
$$X_\tau(t) = (S(t-\tau), E(t-\tau), I(t-\tau), I_a(t-\tau), I_q(t-\tau), H(t-\tau), R(t-\tau)).$$

Then, the Hamiltonian $\mathcal{H}$ of the control problem is defined as,

$$\begin{aligned}
&\mathcal{H}(X, X_\tau, u_1, u_2, u_3, u_4, \lambda_i, t)\\
&\quad = L(E, I, I_a, u_1, u_2, u_3, u_4)\\
&\quad + \lambda_1(t)\left[b(1-u_1(t)) - \beta c(1-u_2(t))S(t)I_a(t) - \frac{\beta c(1-u_2(t))S(t)I(t)}{1+\alpha I(t)} - \mu S(t) + \triangle R(t)\right]\\
&\quad + \lambda_2(t)\left[\beta c(1-u_2(t))S(t)I_a(t) + \frac{\beta c(1-u_2(t))S(t)I(t)}{1+\alpha I(t)} - (\sigma+\mu)E(t)\right]\\
&\quad + \lambda_3(t)\left[\rho_1\sigma E(t) + \phi I_a(t-\tau) - (\theta_I + \mu + \delta)I(t) - u_3(t)I(t)\right]\\
&\quad + \lambda_4(t)\left[\rho_2\sigma E(t) - (\phi_q + \gamma_a + \mu)I_a(t) - \phi I_a(t-\tau)\right]\\
&\quad + \lambda_5(t)\left[\rho_3\sigma E(t) + \phi_q I_a(t) - (\gamma_q + \mu + \delta)I_q(t) - u_4(t)I_q(t)\right]\\
&\quad + \lambda_6(t)\left[\theta_I I(t) - (\gamma + \mu + \delta)H(t) + u_3(t)I(t) + u_4(t)I_q(t)\right]\\
&\quad + \lambda_7(t)\left[\gamma_a I_a(t) + \gamma_q I_q(t) + \gamma H(t) - (\triangle + \mu)R(t) + bu_1(t)\right]
\end{aligned}$$

where, $\lambda_i(t)$ for $i = 1, 2, \ldots, 7$ are adjoint functions which can be determined suitably.

The well known Pontryagin's Maximum Principle states that:

"Consider a delayed control problem with state solution $X(t)$ (where $X_\tau(t) = X(t-\tau)$) and control parameter $u(t)$ then a continuous function $\lambda(t)$ exists on $[0, t_{end}]$, satisfying the three equations given below:

1. State Equation

$$X'(t) = \frac{\partial\mathcal{H}(X, X_\tau, u, \lambda, t)}{\partial\lambda} \tag{5.7}$$

2. The optimality condition

$$0 = \frac{\partial\mathcal{H}(X, X_\tau, u, \lambda, t)}{\partial u} \tag{5.8}$$

3. The adjoint equation

$$-\lambda'(t) = \frac{\partial\mathcal{H}(X, X_\tau, u, \lambda, t)}{\partial X} + \lambda(t+\tau)\frac{\partial\mathcal{H}(X, X_\tau, u, \lambda, t)}{\partial X_\tau}" \tag{5.9}$$

Now, applying Pontryagin's Maximum Principle on the Hamiltonian of the optimal control problem given by (5.2), (5.3) and (5.6), we have the following theorem.

Theorem 8. *Given the optimal control pair $u_i^*(t)$, $i = 1, \dots, 4$ and the optimal state solutions $S^*(t)$, $E^*(t)$, $I^*(t)$, ${I_a}^*(t)$, ${I_q}^*(t)$, $H^*(t)$ and $R^*(t)$, for the optimal control problem given by (5.2), (5.3) and (5.6), there exists adjoint variables $\lambda_j(t)$, $j = 1, \dots, 7$ satisfying,*

$$\begin{aligned}
\frac{d\lambda_1(t)}{dt} =& \lambda_1(t)\Big(\beta c(1-u_2(t))({I_a}^* + \frac{I^*}{1+\alpha I^*}) + \mu\Big) - \lambda_2(t)\beta c(1-u_2(t))({I_a}^* + \frac{I^*}{1+\alpha I^*}),\\
\frac{d\lambda_2(t)}{dt} =& -A_1 + \lambda_2(t)(\sigma+\mu) - \lambda_3(t)\rho_1\sigma - \lambda_4(t)\rho_2\sigma - \lambda_5(t)\rho_3\sigma,\\
\frac{d\lambda_3(t)}{dt} =& -A_2 + (\lambda_1(t)-\lambda_2(t))\frac{\beta c(1-u_2(t))S^*}{(1+\alpha I^*)^2} + \lambda_3(t)(\theta_I+\mu+\delta+u_3(t)) - \lambda_6(t)(\theta_I+u_3(t)),\\
\frac{d\lambda_4(t)}{dt} =& -A_3 + (\lambda_1(t)-\lambda_2(t))\beta c(1-u_2(t))S^* + \lambda_4(t)(\gamma_a+\mu+\phi_q) - \lambda_5(t)\phi_q - \lambda_7(t)\gamma_a\\
&+ \lambda_4(t+\tau)(\lambda_4(t)-\lambda_3(t))\phi,\\
\frac{d\lambda_5(t)}{dt} =& \lambda_5(t)(\gamma_q+\mu+\delta+u_4) - \lambda_6(t)u_4(t) - \lambda_7(t)\gamma_q,\\
\frac{d\lambda_6(t)}{dt} =& \lambda_6(t)(\gamma+\mu+\delta) - \lambda_7(t)\gamma,\\
\frac{d\lambda_7(t)}{dt} =& -\lambda_1(t)\,\Delta + \lambda_7(t)(\Delta+\mu),
\end{aligned} \tag{5.10}$$

with boundary or transversality conditions,

$$\lambda_i(t_{end}) = 0, \ \ i = 1, \dots, 7. \tag{5.11}$$

Moreover, the optimal control pair is:

$$\begin{aligned}
{u_1}^* =& max\left\{0, min\left\{1, \frac{(\lambda_1(t)-\lambda_7(t))b}{2\epsilon_1}\right\}\right\},\\
{u_2}^* =& max\left\{0, min\left\{1, \frac{(\lambda_2(t)-\lambda_1(t))\beta c S^*(t)\left[{I_a}^*(t) + \frac{I(t)}{1+\alpha I^*(t)}\right]}{2\epsilon_2}\right\}\right\},\\
{u_3}^* =& max\left\{0, min\left\{1, \frac{(\lambda_3(t)-\lambda_6(t))I^*(t)}{2\epsilon_3}\right\}\right\},\\
{u_4}^* =& max\left\{0, min\left\{1, \frac{(\lambda_5(t)-\lambda_6(t)){I_q}^*(t)}{2\epsilon_4}\right\}\right\}.
\end{aligned} \tag{5.12}$$

Proof. Here we use condition 3 (Eq. (5.9)) of the Pontryagin's Maximum Principle as follows:

$$\begin{aligned}
\frac{d\lambda_1(t)}{dt} =& -\frac{\partial\mathcal{H}}{\partial S} - \lambda_1(t+\tau)\frac{\partial\mathcal{H}}{\partial S_\tau},\\
\frac{d\lambda_2(t)}{dt} =& -\frac{\partial\mathcal{H}}{\partial E} - \lambda_2(t+\tau)\frac{\partial\mathcal{H}}{\partial E_\tau},\\
\frac{d\lambda_3(t)}{dt} =& -\frac{\partial\mathcal{H}}{\partial I} - \lambda_3(t+\tau)\frac{\partial\mathcal{H}}{\partial I_\tau},\\
\frac{d\lambda_4(t)}{dt} =& -\frac{\partial\mathcal{H}}{\partial I_a} - \lambda_4(t+\tau)\frac{\partial\mathcal{H}}{\partial I_{a\tau}},\\
\frac{d\lambda_5(t)}{dt} =& -\frac{\partial\mathcal{H}}{\partial I_q} - \lambda_5(t+\tau)\frac{\partial\mathcal{H}}{\partial I_{q\tau}},\\
\frac{d\lambda_6(t)}{dt} =& -\frac{\partial\mathcal{H}}{\partial H} - \lambda_6(t+\tau)\frac{\partial\mathcal{H}}{\partial H_\tau},\\
\frac{d\lambda_7(t)}{dt} =& -\frac{\partial\mathcal{H}}{\partial R} - \lambda_7(t+\tau)\frac{\partial\mathcal{H}}{\partial R_\tau}.
\end{aligned} \tag{5.13}$$

The following are obtained by partially differentiating the Hamiltonian $\mathcal{H}$ with respect to the state variables $S(t)$, $E(t)$, $I(t)$, $I_a(t)$, $I_q(t)$, $H(t)$ and $R(t)$, respectively:

$$\begin{aligned}
\frac{\partial\mathcal{H}}{\partial S} =& -\lambda_1(t)\Big(\beta c(1-u_2(t))({I_a}^* + \frac{I^*}{1+\alpha I^*}) + \mu\Big) + \lambda_2(t)\beta c(1-u_2(t))({I_a}^* + \frac{I^*}{1+\alpha I^*}),\\
\frac{\partial\mathcal{H}}{\partial E} =& A_1 - \lambda_2(t)(\sigma+\mu) + \lambda_3(t)\rho_1\sigma + \lambda_4(t)\rho_2\sigma + \lambda_5(t)\rho_3\sigma,\\
\frac{\partial\mathcal{H}}{\partial I} =& A_2 - (\lambda_1(t)-\lambda_2(t))\frac{\beta c(1-u_2(t))S^*}{(1+\alpha I^*)^2} - \lambda_3(t)(\theta_I+\mu+\delta+u_3(t)) + \lambda_6(t)(\theta_I+u_3(t)),\\
\frac{\partial\mathcal{H}}{\partial I_a} =& A_3 - (\lambda_1(t)-\lambda_2(t))\beta c(1-u_2(t))S^* - \lambda_4(t)(\gamma_a+\mu+\phi_q) + \lambda_5(t)\phi_q + \lambda_7(t)\gamma_a,
\end{aligned} \tag{5.14}$$

$$\frac{\partial \mathcal{H}}{\partial I_q} = -\lambda_5(t)(\gamma_q + \mu + \delta + u_4) + \lambda_6(t)u_4(t) + \lambda_7(t)\gamma_q,$$
$$\frac{\partial \mathcal{H}}{\partial H} = -\lambda_6(t)(\gamma + \mu + \delta) + \lambda_7(t)\gamma,$$
$$\frac{\partial \mathcal{H}}{\partial R} = \lambda_1(t) \triangle -\lambda_7(t)(\triangle + \mu),$$

and, the following can be obtained by partially differentiating the Hamiltonian $\mathcal{H}$ with respect to $I_{a\tau} = I_a(t-\tau)$:

$$\frac{\partial \mathcal{H}}{\partial I_{a\tau}} = (\lambda_3(t) - \lambda_4(t))\phi, \tag{5.15}$$

then, we can easily obtain $\frac{d\lambda_i(t)}{dt}$ for $i = 1, 2, ., 7$ as required in the theorem (in (5.10)), by substituting (5.14) and (5.15) into (5.13). In the control problem given by (5.2), (5.3) and (5.6) the final state is free as there is no terminal cost. Therefore, as in [84] we can say that the transversality condition is satisfied and $\lambda_i(t_{end}) = 0$.

Next, using the second condition (Eq. (5.8)) of the Pontryagin's Maximum Principle, we have:

$$\frac{dH}{du_1} = 2\epsilon_1 u_1^*(t) - (\lambda_1(t) - \lambda_7(t))b = 0, \qquad \text{at } u_1 = u_1^*(t),$$
$$\frac{dH}{du_2} = 2\epsilon_2 u_2^*(t) - (\lambda_2(t) - \lambda_1(t))\beta c S^* \left(I_a^* + \frac{I^*}{1+\alpha I^*}\right) = 0, \qquad \text{at } u_2 = u_2^*(t),$$
$$\frac{dH}{du_3} = 2\epsilon_3 u_3^*(t) - (\lambda_3(t) - \lambda_6(t))I^* = 0, \qquad \text{at } u_3 = u_3^*(t),$$
$$\frac{dH}{du_4} = 2\epsilon_4 u_4^*(t) - (\lambda_5(t) - \lambda_6(t))I_q^* = 0, \qquad \text{at } u_4 = u_4^*(t),$$

which gives,

$$u_1{}^*(t) = \frac{(\lambda_1(t) - \lambda_7(t))b}{2\epsilon_1},$$
$$u_2{}^*(t) = \frac{(\lambda_2(t) - \lambda_1(t))\beta c S^*(t)\left[I_a{}^*(t) + \frac{I^*(t)}{1+\alpha I^*(t)}\right]}{2\epsilon_2}$$
$$u_3{}^*(t) = \frac{(\lambda_3(t) - \lambda_6(t))I^*(t)}{2\epsilon_3},$$
$$u_4{}^*(t) = \frac{(\lambda_5(t) - \lambda_6(t))I_q{}^*(t)}{2\epsilon_4}.$$

Using the properties of the admissible set U (defined in (5.1)), $0 \le u_i(t) \le 1$ for $i = 1, 2, 3, 4$. This gives the optimal control pair as required in the theorem (in (5.12)). □

The formula provided by Eq. (5.12) for $u_i^*(t)$, $i = 1, 2, 3, 4$ is known as the characterization of the optimal control pair. We can find the optimal control and the state variables by solving the optimal control problem which consists of the control system (5.2), the adjoint system (5.10), the boundary conditions (5.3) and (5.11), and the characterization of the optimal control pair (5.12). Also, it is observed that second derivative of the Lagrangian with respect to all the control variables $u_i(t)$, $i = 1, 2, 3, 4$ is positive showing that the optimal control problem is minimum at optimal control $u_i{}^*(t)$, $i = 1, 2, 3, 4$.

6. Numerical analysis

In this section, we focus on the numerical analysis of the model (2.1). It is important for a proposed epidemiological model to be consistent with the real world, otherwise all the obtained analytical results turn out to be futile. It is needed to be ensured that if required, after the calibration of the model, the model can be used to forecast the future trends of the disease, so that various mitigation strategies can be adopted beforehand.

In this section, we work with a biologically feasible set of parameters (refer to Table 2) to use the model formulated in previous sections for studying the spread of COVID-19 in China. First, we referred to some published works on COVID-19 in China for a few parameters, like β [59], b (calculated as in [17]), c [52], σ [85], μ (calculated as in [17]) and γ [86], and then the rest parameters are selected using a heuristic approach such that they fit best with the data of active infected cases in China. In addition, we have assumed the initial population set to be as follows:

$$(S, E, I, I_a, I_q, H, R) = (1433783673, 12, 1, 0, 0, 0, 0) \tag{6.1}$$

After fitting the model with the parameters discussed above, R_0 is approximately equal to 3.1 ($R_0 > 1$). Literature like [87–90] are some references that confirmed a similar reproduction number for china. By changing the parameter c from 14.781 to 4.5, we obtain R_0 to be approximately equal to 0.94 ($R_0 < 1$). Now, Fig. 4(a) depicts when $R_0 < 1$ the solution of the system (2.1) converges to DFE, $E_0 = (14 * 10^8, 0, 0, 0, 0, 0, 0)$, which agrees with Theorem 1, suggesting the local asymptotic stability of the system for $R_0 < 1$. While Fig. 4(b) depicts when $R_0 > 1$ the solution converges to endemic equilibrium point,

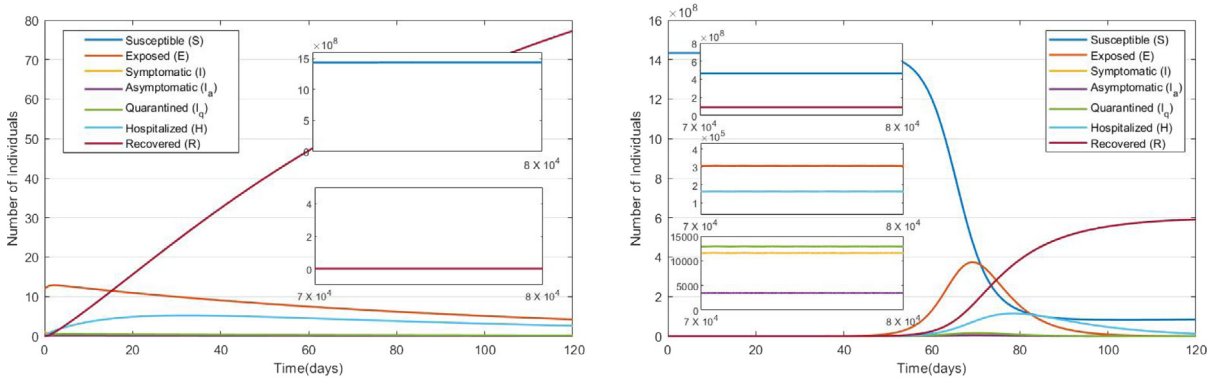

(a) Behaviour of trajectories when $R_0 < 1$

(b) Behaviour of trajectories when $R_0 > 1$

Fig. 4. Time series solution of system (2.1).

$E_1 = (4.6 * 10^8, 3 * 10^5, 11567, 3474, 12917, 1.6 * 10^5, 0.9 * 10^8)$, which complies with Theorem 2, proving the existence of a unique E_1 for $R_0 > 1$.

In the next few sub-sections, we have investigated the sensitivity of different compartments to various model parameters using the One-way Sensitivity Approach [52,91], followed by studying the behaviour of the model in the presence of time delay and control strategies.

6.1. One-way Sensitivity analysis in the absence of control and delay

In this section we have used the One-Way Sensitivity analysis approach to analyse the behaviour of various classes when only a single parameter changes, and the rest of the parameters are still at their base value.

Such an analysis on an epidemiological model helps in predicting various steps that can be taken instantly to cope with the spreading disease at the initial stage itself, while proper treatment and medication for the disease are being figured out. We have worked with factors like β, c, σ, ϕ and θ_I, because these are some of the parameters that can be controlled in real sense by social distancing, imposing lockdown, precautionary measures and regular testing being conducted by the government. Fig. 5 depicts how the seven populations of the model change in response to the change in probability of transmission per contact β. Fig. 5(c) depicts the trajectories at the base level of β. It can be observed, that with a decrease in β the trajectories shift towards the right (see Fig. 5(b)), indicating that in the presence of lower levels of β, the spread of the infection will be delayed.

While with an increase in β, the trajectories shift towards left (see Fig. 5(d)), indicating that the greater the level of β, the earlier the spread begins. Further, it can be observed that the height of the curve for Exposed compartment change with the changing β. The peak is lower when β is decreased while it is higher when β is increased, indicating that the higher the probability of transmission per contact, more the number of Exposed individuals and hence greater the infection. It can also be noted from Fig. 5 that as β increases the rate at which the susceptible population decrease in the system keeps on increasing. For instance, when $\beta = 5.62 * 10^{-10}$ (in Fig. 5(c)) the susceptible population start falling around the 50th day, whereas, when β is increased to $6 * 10^{-10}$ (in Fig. 5(d)) the susceptible population start falling around the 40th day itself. Similarly, Fig. 5(a) depicts that at zero probability of transmission of disease upon contact within the population, the susceptible population thrives at positive levels and there is no infection in the system due to which the trajectories of all other compartments rest at zero. While it is difficult to achieve $\beta = 0$, it can be brought to lower levels by taking proper precautionary measures. By the above discussion, it can be understood why wearing masks has been employed as a mitigation strategy against COVID-19 all across the globe.

Fig. 6 shows how various compartments behave in the presence of changing parameters. Fig. 6(c) shows that with increase in ϕ, exposed individuals are decreased. This is because ϕ is the rate with which asymptomatic people start showing symptoms and shift to the I class, and hence due to the reduction of asymptomatic individuals there are less accidental cases of a susceptible individual coming into contact of an infective individual without knowing about it. Further, it can be seen from Fig. 6(b) that higher the rate with which exposed population become infected, more the level of symptomatic individuals in the system. And Fig. 6(d) depicts how the number of recovered individuals increase with the increase in θ_I, which is the rate of hospitalization of I individuals. Therefore, there should be more focus on medical facilities. Also, temporary lockdowns can significantly help in reducing the infection as it leads to a reduced contact rate. It can be observed from Fig. 6(a) that when c is equal to 0, the infected population is at zero levels. This mean that if the people are not coming in contact with each other at all, the disease will stop spreading due to the lack of new host bodies for the virus. But, it is next to impossible to achieve $c = 0$ permanently, because measures like lockdown drastically affect the economy and this is only a short term solution.

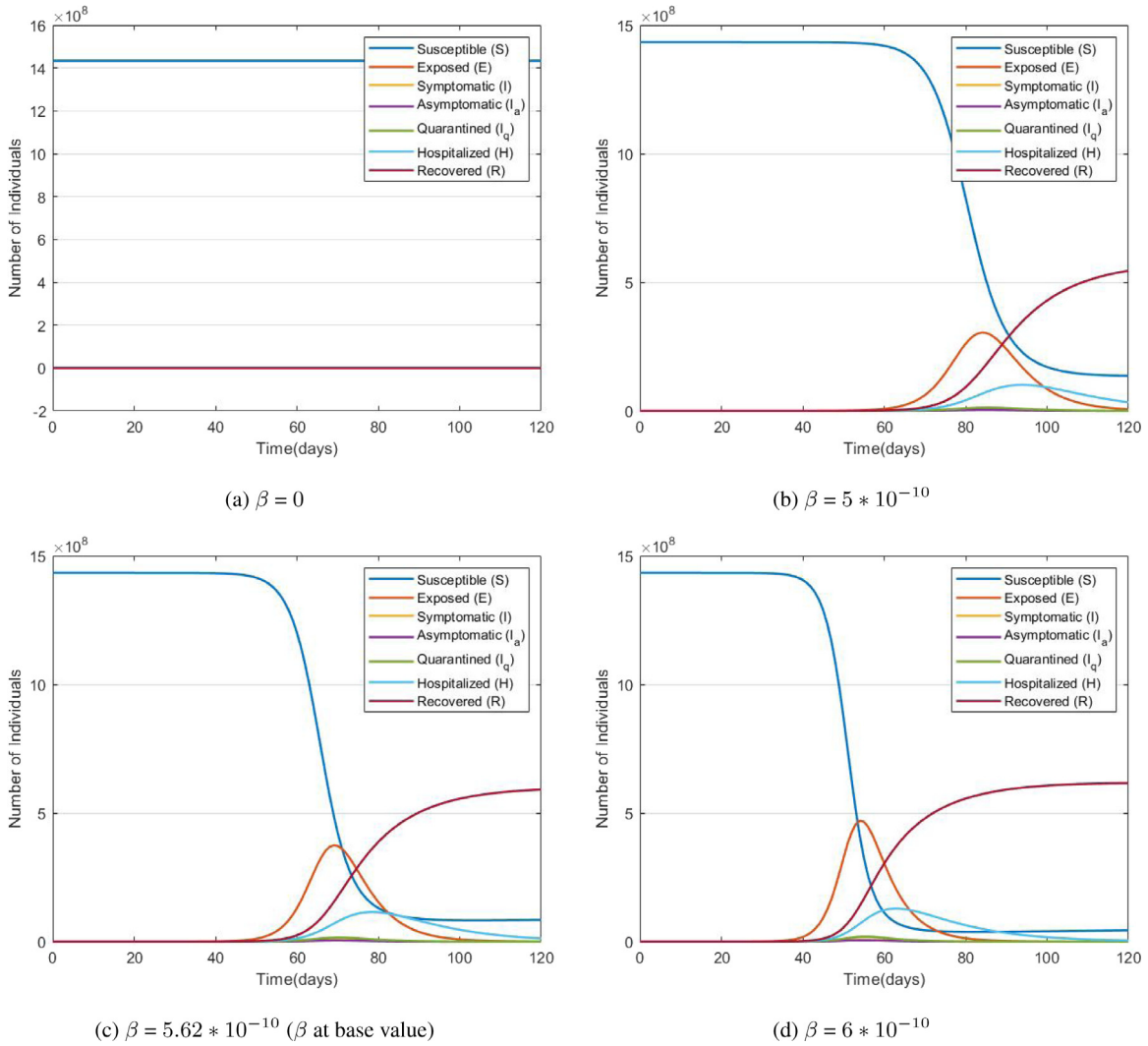

(a) $\beta = 0$

(b) $\beta = 5 * 10^{-10}$

(c) $\beta = 5.62 * 10^{-10}$ (β at base value)

(d) $\beta = 6 * 10^{-10}$

Fig. 5. Behaviour of model in response to changing β.

6.2. *Effect of control parameters and delay parameter*

This sub-section, discusses the numerical simulations on the controlled dynamics of all state variables based on the set of parameters provided in the Table 2. We use Euler method to study and compare the controlled and uncontrolled model presented above graphically. Using MATLAB we have obtained the graphical results with varying conditions with the combination of both delay parameter τ and control parameters u_1, u_2, u_3 and u_4. We have assigned values to all the parameters, initialized the values of state variables and the weight constants provided in the objective functional. All the state equations have been solved with the help of forward Euler method and then the adjoint equations have been solved by backward Euler method. Next we have control updates for u_1, u_2, u_3 and u_4 using weighted convex combinations. We have done our graphical interpretation for 120 days and analysed the behaviour of all the state variables.

In Fig. 7 we have discussed the behaviour of different compartments under various combinations of delay and controllers. As our analytical results suggest implementation of control strategies and a reduction in the delay factor can significantly reduce the infection in the population, therefore, discussing numerical simulations of model in presence of controllers and delay is very important. If we compare Fig. 7(a) with Fig. 7(b), and Fig. 7(c) with Fig. 7(d) we can observe the impact of control strategies very clearly. In the absence of any control strategies (in Figs. 7(a) and 7(c)), we can see that the peaks of infective classes are considerably high. For instance, in Fig. 7(a) (where we have no control strategies in the system) the number of exposed, symptomatic, asymptomatic, quarantined and hospitalized individuals have peaked to approximately $4 * 10^8$, $1.5 * 10^7$, $0.5 * 10^7$, $1.8 * 10^7$ and $1.2 * 10^8$, respectively while in Fig. 7(b) (where control strategies have been implemented) the numbers are only 2500, 100, 30, 100 and 700, respectively. A similar positive effect of controllers can be observed in the presence of delay as well, if we do a similar

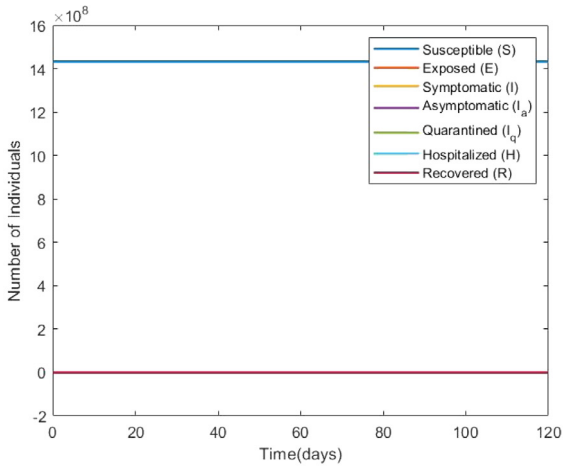

(a) Behavious of the model in case of $c = 0$

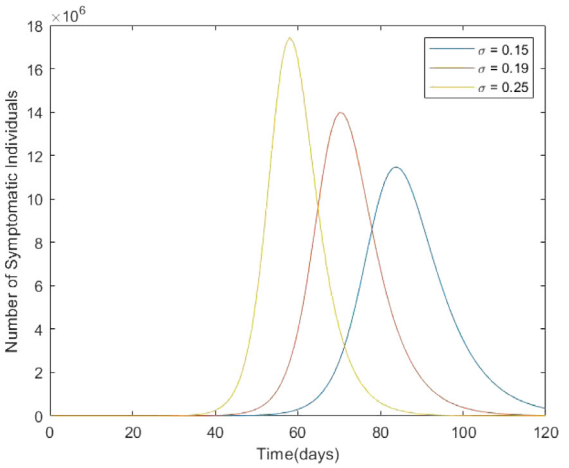

(b) Sensitivity of Symptomatic compartment to σ

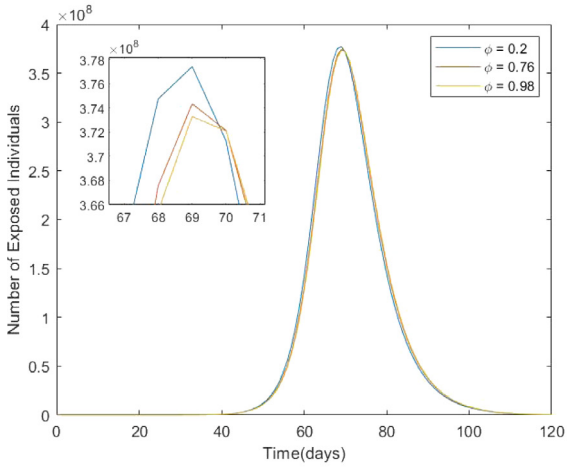

(c) Sensitivity of Exposed compartment to ϕ

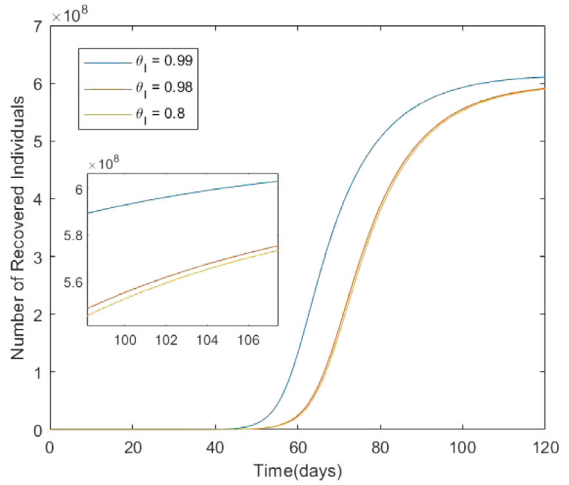

(d) Sensitivity of Recovered compartment to θ_I

Fig. 6. Behaviour of some compartments in response to changing parameters.

comparison of Figs. 7(c) and 7(d). These observations suggest that, control strategies can significantly help to control the spread of the disease and in their absence this spread can go out of hands. A delay in the development of symptoms in some exposed individuals (who are currently thought of as asymptomatic) can also speed up the spread of infection. The longer an individual remains asymptomatic (and hence unrecognizable), the lesser would be the inhibition from susceptible class and more individuals will keep on getting infected. Comparing Fig. 7(a) with Fig. 7(c) and Fig. 7(b) with Fig. 7(d), we can clearly see how the peaks in the absence of delay are significantly low and the number of recovered individuals are comparatively higher. Fig. 7 also suggests that the best strategy is when there are non-zero controllers and an absence of delay (see Fig. 7(b)). Delay can be controlled to some extent by doing mass testings but it is impossible to achieve a condition where delay is exactly zero. Therefore, the next best situation, i.e. a combination of non-zero controllers and non-zero delay within certain limits (see Fig. 7(d)), turns out to be the most sensible strategy to cope with an epidemic. Also, it is worthwhile to note the worst case scenario in Fig. 7(c) where we have zero controllers and a non-zero delay, which is the case during the initial stage of any epidemic.

Talking about the best and the worst combinations, Fig. 8(a) depicts the behaviour of the susceptible class in the two scenarios. We can see how in the presence of delay and absence of controllers (green curve in Fig. 8(a)) the susceptible class undergo a steep fall but in the absence of delay and presence of controllers (yellow curve in Fig. 8(a)) the susceptible population is stable. It is to be noted that, it may seem as if the susceptible population (the yellow curve in Fig. 8(a)) is constant and do not change at all in the presence of controllers and absence of delay, but it is misleading as Fig. 8(b) clearly shows a decrease in the susceptible population. However, this decrease is very small as in this case the infection is very low (refer to Fig. 7(b)) and as a result the susceptible population is thriving and is not affected much. However, as discussed before this is only an ideal situation and not a realistic one. In reality, we have seen that it takes a few more days (than the ideal incubation period) to develop symptoms after exposure with

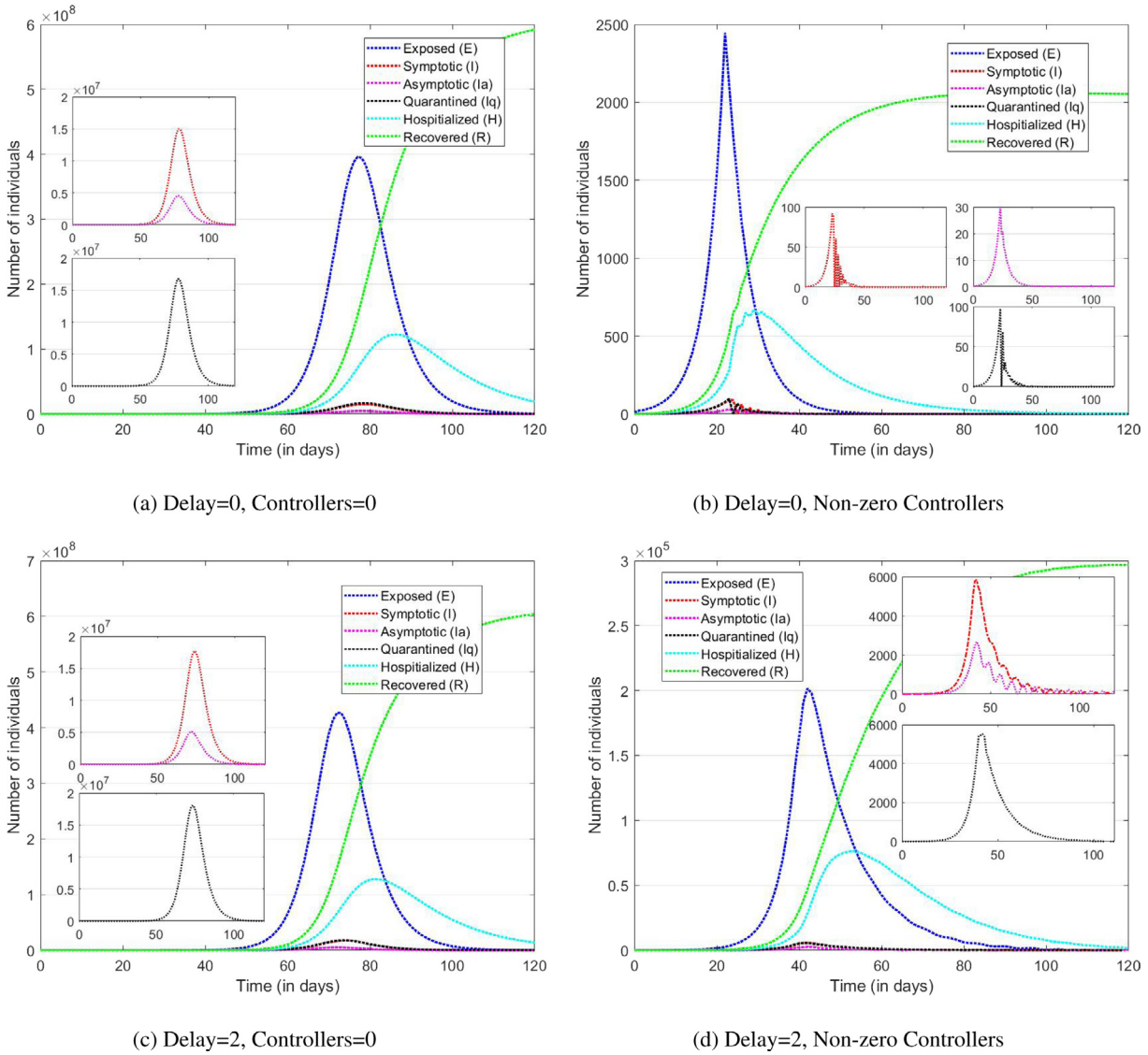

(a) Delay=0, Controllers=0

(b) Delay=0, Non-zero Controllers

(c) Delay=2, Controllers=0

(d) Delay=2, Non-zero Controllers

Fig. 7. Behaviour of E, I, I_a, I_q, H and R population under various combinations of delay and controllers.

a COVID-positive person. China is the only country that could bring the situation under control in a very short period, when the country suffered at the hands of COVID-19. Therefore, it is worthwhile to study the case of China and talk about the possible reasons that helped in controlling the disease rapidly.

Fig. 9 discusses the possible control strategies that could be implemented to deal with this pandemic. The figure is basically a numerical solution of the optimal control pair obtained in Section 5.4 (see Eq. (5.12)) and is a pictorial representation of the time dependent solution. It tells the levels of control strategies implemented in order to cope with the COVID-19 disease. Fig. 9 depicts the variation in the effectiveness of control strategies over time. Furthermore, the graph shows which controls may be used and the amount of intensity that can be applied to the controllers in order to prevent the spread of COVID-19 infection in 120 days. The fluctuations in the control strategy u_1 imply that it is of utmost importance to keep track of the new recruited susceptible individuals, then they will not come in contact with others and will be removed from the stages of infection for the entire period. Similarly, the fluctuations in u_2 imply that it is mandatory to adopt preventive measures (such as social distancing, using mask, sanitizing, etc.) which can be implemented by raising awareness of the issue through advertising that stresses the value of preventative actions in battling the disease. Therefore, $u_3(t)$ is applied on the 'Symptomatic' class and refers to the government initiative of tracking and hospitalizing more and more individuals showing symptoms. Additionally, due to a lack of hospital beds, even those who desired to be hospitalized were unable to do so. This can also be done by putting up helplines, apps, and other means of helping people locate hospitals with open beds. In real life government set up helplines, created apps to aid people in getting vacant hospital bed. This is how u_3 was realized in real life. Therefore, the fourth control variable $u_4(t)$, is applied on the 'Quarantined' class and refers

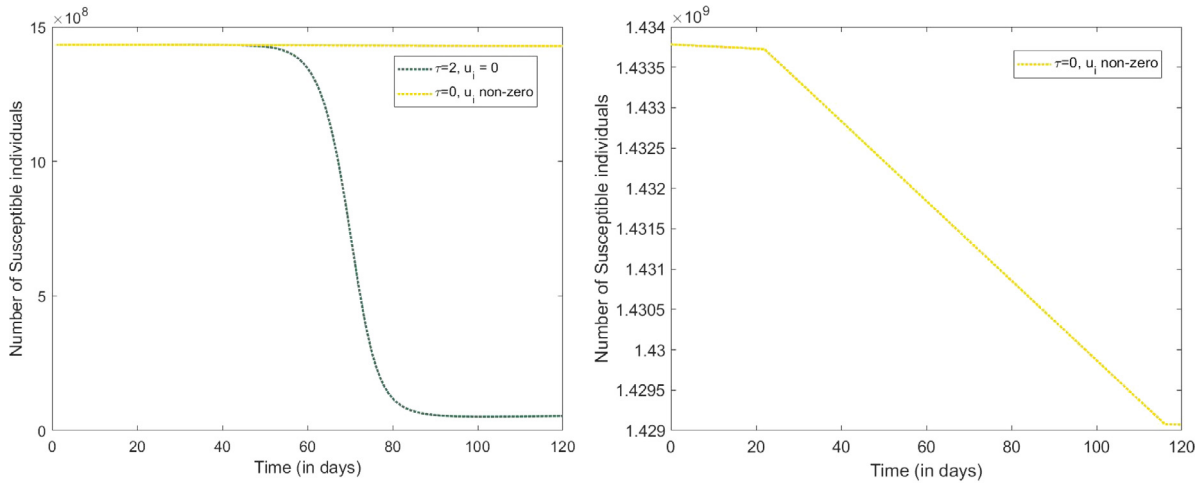

(a) τ=2, u_i=0 and τ=0, u_i not equal to zero

(b) τ=0, u_i not equal to 0

Fig. 8. Behaviour of Susceptible (S) population under various combinations of τ and u. (For interpretation of the references to colour in this figure legend, the reader is referred to the web version of this article.)

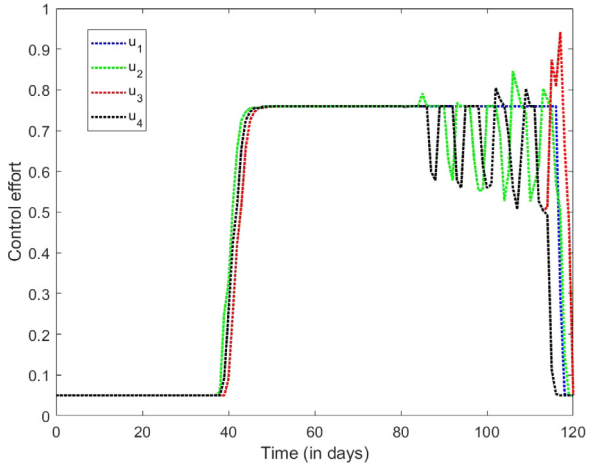

Fig. 9. Controller performance when $\tau = 2$.

to the frequent monitoring of quarantined individuals by government, so that they remain in quarantine till they recover and in case their symptoms deteriorate, provide necessary hospitalization facilities. A real-life application of $u_4(t)$ is how government kept a data base of all infected individuals and also reached them on a regular basis via calls, in order to keep a check on their condition.

Now, we compare the results of our model with the actual data from China. We use the data of active infected cases from [92] to numerically simulate our model. Model parameters are same as in Table 2. We have fitted our model with real time data of active infected count from China's population and compared the predictions of our model with actual numbers. This analysis has been done to give a basic yet viable and informative model for the future predictions, and depict the viability of regulatory and precautionary measures.

In Fig. 10(b) the actual data of active infected individuals in China is represented by the green curve. The red, yellow, blue and purple curves represent the trajectory of active infected individuals predicted by our model in the presence of controllers and a delay of $\tau = 0$, $\tau = 1$, $\tau = 2$ and $\tau = 3$, respectively. It can be observed that the numbers predicted by the model are close to the actual numbers, if we assume that there was a delay of 2 days in the development of symptoms (or identifying asymptomatic individuals) when the infection spread in China. Fig. 10(a) depicts that in the absence of strict control strategies China could have witnessed active infected cases as high as 130 million. But as can be seen in Fig. 10(b), the maximum number of active infected cases were only around 60,000 which implies China had a very thoughtful combination of control strategies and was very quick in imposing restrictions and doing aggressive mass testing. This mass testing really helped to reduce the delay in identifying asymptomatic persons and consequently reducing infection. Thus, we have verified the accuracy and effectiveness of our model, equipped with

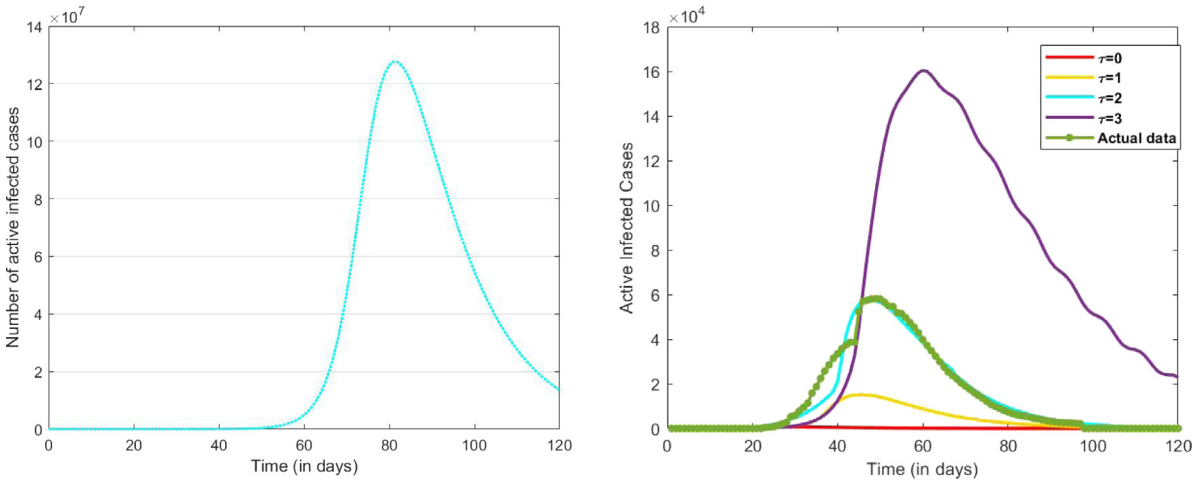

(a) Active infected cases when u_i=0, τ=2

(b) Active infected cases when $u_i \neq 0$, τ=0,1,2,3

Fig. 10. Comparison with real data from China. (For interpretation of the references to colour in this figure legend, the reader is referred to the web version of this article.)

control strategies and time delay, which fits best with real data. Therefore, when both time delay and optimal control parameters are introduced into the model there is a significant reduction in the spread of the infection.

7. Discussion and conclusion

In this study, we looked into the epidemiological model, with the help of an $S-E-I-H-R-S$ compartmental model. Although the dynamics of many communicable diseases, including influenza, Ebola virus disease, measles, tuberculosis, etc., might be studied using this model. However, since the entire world is now battling COVID-19, we in our study take this particular scenario into consideration. We obtained some very important and useful analytical results, for instance the basic reproduction number (R_0), the disease-free (E_0) and endemic (E_1) equilibria. Then we derived the conditions for which E_0 and E_1 are stable based on R_0. We established that $R_0 < 1$ would imply local asymptotic stability of E_0, as was seen in Fig. 4(a), where the system could be seen converging to E_0 when $R_0 < 1$. For system (2.1), it was seen in Fig. 4(b) that the system converged to E_1 for $R_0 > 1$. We also derived conditions for Hopf bifurcates at E_1 for the bifurcation parameter $\tau = \tau_0$. We discussed the importance of τ as bifurcation parameter and dependence of the epidemic transmission on length of the delayed period, τ. It was proved that if the delay is beyond a certain critical level, τ_0, the endemic equilibrium point looses its stability. The effect of parameters on R_0 was studied using sensitivity analysis and it was seen in Fig. 2, how R_0 is highly sensitive to certain parameters like β and c. For instance, Fig. 5 suggested, with a decrease in β infection is reduced in the system. Similarly, Fig. 6(a) suggested in case of zero contact rate there is no infection in the system. Hence, measures like social distancing, lockdowns and using face masks can be employed to bring down the values of these parameters, hence reducing the spread of the infection. Similarly, Fig. 6(c) suggested, that if testing is being regularly conducted, more and more asymptomatic individuals can be identified, which can help in reducing cases of new exposed individuals.

Also, we discussed various control measures to cope with the disease. We investigated the following four non-pharmaceutical precautionary and preventive control strategies for coping with novel coronavirus: (1) Home-isolation of the susceptible individuals; (2) Taking preventive measures; (3) Government intervention to track and hospitalize symptomatic individuals; and (4) Government intervention to monitor and hospitalize quarantine individuals, if necessary. Our main focus was to relatively set up an optimal control problem and find an optimal solution to significantly reduce infection and increase the count of recovered individuals. We first proved the existence of optimal control pair u_i^*, $i = 1, 2, 3, 4$ and then to achieve our goal, we used the Pontryagin's maximum principle to obtain the optimal solution. In addition, the significant numerical findings of time delayed model were mathematically verified using MATLAB. We compared combination of with and without controls (see Fig. 7) and with and without time lag (see Fig. 7). It was analysed that a combination of all the controllers (see Fig. 9) can slow down the growth of infected individuals and prevent any outbreak. We showed through the graphical results that control strategies help in increasing the susceptible individuals and decreasing the infection. Also, with increasing time delay, infection kept on increasing (see Fig. 10(b)), which was due to the increased delay in the development of symptoms in some asymptomatic individuals and hence increased chances of contact with asymptomatic individuals.

Next, we compared the predictions of our model with the real-time data from China. Our estimations fitted well with the real data (see Fig. 10(b)). It was deduced that with a combination of control strategies for around 120 days in China, the count of infected individuals decreased. Thus, we can conclude that in order to reduce the spread of infection, imposing strict non-pharmaceutical measures (like home isolation, social distancing, increased hospitalization facilities and isolation) as control strategies can prove to

be viable. Since, our model fits well with the COVID-19 data from China, hence our model is realistic. Applying control policies on epidemiological model provides a great help to the researchers in making necessary future predictions. Therefore, until people are properly vaccinated all over the globe, control measures will play an important role in dealing with the disease. Although, our findings suggest that non-pharmaceutical interventions like self-isolation of susceptible individuals, reduced contact with infected individuals, and government monitoring can help in reducing the rate of transmission and bringing down the disease-induced mortality rate, but the success of these strategies will only depend upon their proper implementation.

Declaration of competing interest

The authors declare that they have no known competing financial interests or personal relationships that could have appeared to influence the work reported in this paper.

Data availability

Data will be made available on reasonable request.

Acknowledgement

The first author thanks the IoE, University of Delhi for the faculty research program grant 2020.

Appendix

Assuming the following notations in the determinant before Eq. (3.16) :

$$
\begin{aligned}
a_{11} &= -\mu - \beta c\left(I_a^{**} + \frac{I^{**}}{(1+\alpha I^{**})^2}\right)\\
a_{13} &= \frac{-\beta c S^{**}}{(1+\alpha I^{**})^2}\\
a_{14} &= -\beta c S^{**}\\
a_{17} &= \triangle\\
a_{21} &= \beta c\left(I_a^{**} + \frac{I^{**}}{(1+\alpha I^{**})^2}\right)\\
a_{22} &= -(\sigma+\mu)\\
a_{23} &= -a_{13}\\
a_{24} &= -a_{14}\\
a_{32} &= \rho_1\sigma\\
a_{33} &= -(\theta_I+\mu+\delta)\\
a_{34} &= \phi e^{-\lambda\tau}\\
a_{42} &= \rho_2\sigma\\
a_{44} &= -(\phi_q+\gamma_a+\mu) - \phi e^{-\lambda\tau}\\
a_{52} &= \rho_3\sigma\\
a_{54} &= \phi_q\\
a_{55} &= -(\gamma_q+\mu+\delta)\\
a_{63} &= \theta_I\\
a_{66} &= -(\gamma+\mu+\delta)\\
a_{74} &= \gamma_a\\
a_{75} &= \gamma_q\\
a_{76} &= \gamma\\
a_{77} &= -(\triangle+\mu)
\end{aligned}
\tag{A.1}
$$

we have the values for $p_0,\dots,p_6$ and $q_0,\dots,q_6$ as below:

$$
\begin{aligned}
&[p_0+q_0; p_1+q_1; p_2+q_2; p_3+q_3; p_4+q_4; p_5+q_5; p_6+q_6;] =\\
&[a_{11}a_{13}a_{34}a_{42}a_{55}a_{66}a_{77} - a_{11}a_{13}a_{32}a_{44}a_{55}a_{66}a_{77} - a_{11}a_{14}a_{33}a_{42}a_{55}a_{66}a_{77}\\
&+ a_{11}a_{22}a_{33}a_{44}a_{55}a_{66}a_{77}\\
&- a_{13}a_{21}a_{32}a_{44}a_{55}a_{66}a_{77} + a_{13}a_{21}a_{34}a_{42}a_{55}a_{66}a_{77} - a_{14}a_{21}a_{33}a_{42}a_{55}a_{66}a_{77}
\end{aligned}
$$

$$
\begin{aligned}
&+ a_{17}a_{21}a_{32}a_{44}a_{55}a_{63}a_{76} + a_{17}a_{21}a_{33}a_{42}a_{54}a_{66}a_{75} - a_{17}a_{21}a_{33}a_{42}a_{55}a_{66}a_{74}\\
&- a_{17}a_{21}a_{33}a_{44}a_{52}a_{66}a_{75} - a_{17}a_{21}a_{34}a_{42}a_{55}a_{63}a_{76}, a_{11}a_{13}a_{32}a_{44}a_{55}a_{66}\\
&- a_{11}a_{13}a_{34}a_{42}a_{55}a_{66} + a_{11}a_{14}a_{33}a_{42}a_{55}a_{66} - a_{11}a_{22}a_{33}a_{44}a_{55}a_{66} + a_{13}a_{21}a_{32}a_{44}a_{55}a_{66} - a_{13}a_{21}a_{34}a_{42}a_{55}a_{66}\\
&+ a_{14}a_{21}a_{33}a_{42}a_{55}a_{66} + a_{11}a_{13}a_{32}a_{44}a_{55}a_{77} - a_{11}a_{13}a_{34}a_{42}a_{55}a_{77} + a_{11}a_{14}a_{33}a_{42}a_{55}a_{77} - a_{11}a_{22}a_{33}a_{44}a_{55}a_{77}\\
&+ a_{13}a_{21}a_{32}a_{44}a_{55}a_{77} - a_{13}a_{21}a_{34}a_{42}a_{55}a_{77} + a_{14}a_{21}a_{33}a_{42}a_{55}a_{77} - a_{17}a_{21}a_{33}a_{42}a_{54}a_{75}\\
&+ a_{17}a_{21}a_{33}a_{42}a_{55}a_{74} + a_{17}a_{21}a_{33}a_{44}a_{52}a_{75} + a_{11}a_{13}a_{32}a_{44}a_{66}a_{77}\\
&- a_{11}a_{13}a_{34}a_{42}a_{66}a_{77} + a_{11}a_{14}a_{33}a_{42}a_{66}a_{77} - a_{11}a_{22}a_{33}a_{44}a_{66}a_{77}\\
&+ a_{13}a_{21}a_{32}a_{44}a_{66}a_{77} - a_{13}a_{21}a_{34}a_{42}a_{66}a_{77} + a_{14}a_{21}a_{33}a_{42}a_{66}a_{77} - a_{17}a_{21}a_{32}a_{44}a_{63}a_{76}\\
&+ a_{17}a_{21}a_{33}a_{42}a_{66}a_{74} + a_{17}a_{21}a_{34}a_{42}a_{63}a_{76} + a_{11}a_{13}a_{32}a_{55}a_{66}a_{77} - a_{11}a_{22}a_{33}a_{55}a_{66}a_{77}\\
&+ a_{13}a_{21}a_{32}a_{55}a_{66}a_{77} - a_{17}a_{21}a_{32}a_{55}a_{63}a_{76} + a_{17}a_{21}a_{33}a_{52}a_{66}a_{75} + a_{11}a_{14}a_{42}a_{55}a_{66}a_{77}\\
&- a_{11}a_{22}a_{44}a_{55}a_{66}a_{77} + a_{14}a_{21}a_{42}a_{55}a_{66}a_{77} - a_{17}a_{21}a_{42}a_{54}a_{66}a_{75}\\
&+ a_{17}a_{21}a_{42}a_{55}a_{66}a_{74} + a_{17}a_{21}a_{44}a_{52}a_{66}a_{75} - a_{11}a_{33}a_{44}a_{55}a_{66}a_{77} + a_{13}a_{32}a_{44}a_{55}a_{66}a_{77} - a_{13}a_{34}a_{42}a_{55}a_{66}a_{77}\\
&+ a_{14}a_{33}a_{42}a_{55}a_{66}a_{77} - a_{22}a_{33}a_{44}a_{55}a_{66}a_{77}, a_{11}a_{13}a_{34}a_{42}a_{55} - a_{11}a_{13}a_{32}a_{44}a_{55} - a_{11}a_{14}a_{33}a_{42}a_{55}\\
&+ a_{11}a_{22}a_{33}a_{44}a_{55} - a_{13}a_{21}a_{32}a_{44}a_{55}\\
&+ a_{13}a_{21}a_{34}a_{42}a_{55} - a_{14}a_{21}a_{33}a_{42}a_{55} - a_{11}a_{13}a_{32}a_{44}a_{66} + a_{11}a_{13}a_{34}a_{42}a_{66} - a_{11}a_{14}a_{33}a_{42}a_{66}\\
&+ a_{11}a_{22}a_{33}a_{44}a_{66} - a_{13}a_{21}a_{32}a_{44}a_{66} + a_{13}a_{21}a_{34}a_{42}a_{66} - a_{14}a_{21}a_{33}a_{42}a_{66} - a_{11}a_{13}a_{32}a_{44}a_{77} - a_{11}a_{13}a_{32}a_{55}a_{66}\\
&+ a_{11}a_{13}a_{34}a_{42}a_{77} - a_{11}a_{14}a_{33}a_{42}a_{77} + a_{11}a_{22}a_{33}a_{44}a_{77} + a_{11}a_{22}a_{33}a_{55}a_{66} - a_{13}a_{21}a_{32}a_{44}a_{77} - a_{13}a_{21}a_{32}a_{55}a_{66}\\
&+ a_{13}a_{21}a_{34}a_{42}a_{77} - a_{14}a_{21}a_{33}a_{42}a_{77} - a_{17}a_{21}a_{33}a_{42}a_{74} - a_{11}a_{13}a_{32}a_{55}a_{77} - a_{11}a_{14}a_{42}a_{55}a_{66} + a_{11}a_{22}a_{33}a_{55}a_{77}\\
&+ a_{11}a_{22}a_{44}a_{55}a_{66} - a_{13}a_{21}a_{32}a_{55}a_{77} - a_{14}a_{21}a_{42}a_{55}a_{66} - a_{17}a_{21}a_{33}a_{52}a_{75} - a_{11}a_{13}a_{32}a_{66}a_{77} - a_{11}a_{14}a_{42}a_{55}a_{77}\\
&+ a_{11}a_{22}a_{33}a_{66}a_{77} + a_{11}a_{22}a_{44}a_{55}a_{77} + a_{11}a_{33}a_{44}a_{55}a_{66} - a_{13}a_{21}a_{32}a_{66}a_{77} - a_{14}a_{21}a_{42}a_{55}a_{77}\\
&+ a_{17}a_{21}a_{32}a_{63}a_{76} + a_{17}a_{21}a_{42}a_{54}a_{75} - a_{17}a_{21}a_{42}a_{55}a_{74} - a_{17}a_{21}a_{44}a_{52}a_{75} - a_{11}a_{14}a_{42}a_{66}a_{77}\\
&- a_{13}a_{32}a_{44}a_{55}a_{66} + a_{13}a_{34}a_{42}a_{55}a_{66} - a_{14}a_{33}a_{42}a_{55}a_{66} + a_{11}a_{22}a_{44}a_{66}a_{77} + a_{11}a_{33}a_{44}a_{55}a_{77} - a_{14}a_{21}a_{42}a_{66}a_{77}\\
&- a_{17}a_{21}a_{42}a_{66}a_{74} + a_{22}a_{33}a_{44}a_{55}a_{66} - a_{13}a_{32}a_{44}a_{55}a_{77} + a_{13}a_{34}a_{42}a_{55}a_{77} - a_{14}a_{33}a_{42}a_{55}a_{77}\\
&+ a_{11}a_{22}a_{55}a_{66}a_{77} + a_{11}a_{33}a_{44}a_{66}a_{77} - a_{17}a_{21}a_{52}a_{66}a_{75} + a_{22}a_{33}a_{44}a_{55}a_{77} - a_{13}a_{32}a_{44}a_{66}a_{77} + a_{13}a_{34}a_{42}a_{66}a_{77} - a_{14}a_{33}a_{42}a_{66}a_{77}\\
&+ a_{11}a_{33}a_{55}a_{66}a_{77} + a_{22}a_{33}a_{44}a_{66}a_{77} - a_{13}a_{32}a_{55}a_{66}a_{77} + a_{11}a_{44}a_{55}a_{66}a_{77} + a_{22}a_{33}a_{55}a_{66}a_{77}\\
&- a_{14}a_{42}a_{55}a_{66}a_{77} + a_{22}a_{44}a_{55}a_{66}a_{77} + a_{33}a_{44}a_{55}a_{66}a_{77}, a_{11}a_{13}a_{32}a_{44} - a_{11}a_{13}a_{34}a_{42}\\
&+ a_{11}a_{14}a_{33}a_{42} - a_{11}a_{22}a_{33}a_{44} + a_{13}a_{21}a_{32}a_{44} - a_{13}a_{21}a_{34}a_{42} + a_{14}a_{21}a_{33}a_{42} + a_{11}a_{13}a_{32}a_{55} - a_{11}a_{22}a_{33}a_{55}\\
&+ a_{13}a_{21}a_{32}a_{55} + a_{11}a_{13}a_{32}a_{66} + a_{11}a_{14}a_{42}a_{55}\\
&- a_{11}a_{22}a_{33}a_{66} - a_{11}a_{22}a_{44}a_{55} + a_{13}a_{21}a_{32}a_{66} + a_{14}a_{21}a_{42}a_{55} + a_{11}a_{13}a_{32}a_{77}\\
&+ a_{11}a_{14}a_{42}a_{66} - a_{11}a_{22}a_{33}a_{77} - a_{11}a_{22}a_{44}a_{66} - a_{11}a_{33}a_{44}a_{55} + a_{13}a_{21}a_{32}a_{77} + a_{14}a_{21}a_{42}a_{66}\\
&+ a_{11}a_{14}a_{42}a_{77} + a_{13}a_{32}a_{44}a_{55} - a_{13}a_{34}a_{42}a_{55}\\
&+ a_{14}a_{33}a_{42}a_{55} - a_{11}a_{22}a_{44}a_{77} - a_{11}a_{22}a_{55}a_{66} - a_{11}a_{33}a_{44}a_{66} + a_{14}a_{21}a_{42}a_{77} + a_{17}a_{21}a_{42}a_{74} - a_{22}a_{33}a_{44}a_{55}\\
&+ a_{13}a_{32}a_{44}a_{66} - a_{13}a_{34}a_{42}a_{66} + a_{14}a_{33}a_{42}a_{66} - a_{11}a_{22}a_{55}a_{77} - a_{11}a_{33}a_{44}a_{77} - a_{11}a_{33}a_{55}a_{66}\\
&+ a_{17}a_{21}a_{52}a_{75} - a_{22}a_{33}a_{44}a_{66} + a_{13}a_{32}a_{44}a_{77} + a_{13}a_{32}a_{55}a_{66} - a_{13}a_{34}a_{42}a_{77} + a_{14}a_{33}a_{42}a_{77} - a_{11}a_{22}a_{66}a_{77}\\
&- a_{11}a_{33}a_{55}a_{77} - a_{11}a_{44}a_{55}a_{66} - a_{22}a_{33}a_{44}a_{77} - a_{22}a_{33}a_{55}a_{66} + a_{13}a_{32}a_{55}a_{77} + a_{14}a_{42}a_{55}a_{66} - a_{11}a_{33}a_{66}a_{77}\\
&- a_{11}a_{44}a_{55}a_{77} - a_{22}a_{33}a_{55}a_{77} - a_{22}a_{44}a_{55}a_{66} + a_{13}a_{32}a_{66}a_{77} + a_{14}a_{42}a_{55}a_{77} - a_{11}a_{44}a_{66}a_{77} - a_{22}a_{33}a_{66}a_{77} - a_{22}a_{44}a_{55}a_{77}\\
&- a_{33}a_{44}a_{55}a_{66} + a_{14}a_{42}a_{66}a_{77} - a_{11}a_{55}a_{66}a_{77} - a_{22}a_{44}a_{66}a_{77} - a_{33}a_{44}a_{55}a_{77} - a_{22}a_{55}a_{66}a_{77} - a_{33}a_{44}a_{66}a_{77}\\
&- a_{33}a_{55}a_{66}a_{77} - a_{44}a_{55}a_{66}a_{77}, a_{11}a_{22}a_{33} - a_{11}a_{13}a_{32} - a_{13}a_{21}a_{32} - a_{11}a_{14}a_{42} + a_{11}a_{22}a_{44} - a_{14}a_{21}a_{42} + a_{11}a_{22}a_{55}\\
&+ a_{11}a_{33}a_{44} - a_{13}a_{32}a_{44} + a_{13}a_{34}a_{42} - a_{14}a_{33}a_{42} + a_{11}a_{22}a_{66} + a_{11}a_{33}a_{55} + a_{22}a_{33}a_{44} - a_{13}a_{32}a_{55} + a_{11}a_{22}a_{77}\\
&+ a_{11}a_{33}a_{66} + a_{11}a_{44}a_{55} + a_{22}a_{33}a_{55} - a_{13}a_{32}a_{66} - a_{14}a_{42}a_{55} + a_{11}a_{33}a_{77} + a_{11}a_{44}a_{66} + a_{22}a_{33}a_{66}\\
&+ a_{22}a_{44}a_{55} - a_{13}a_{32}a_{77} - a_{14}a_{42}a_{66} + a_{11}a_{44}a_{77} + a_{11}a_{55}a_{66} + a_{22}a_{33}a_{77} + a_{22}a_{44}a_{66} + a_{33}a_{44}a_{55}\\
&- a_{14}a_{42}a_{77} + a_{11}a_{55}a_{77} + a_{22}a_{44}a_{77} + a_{22}a_{55}a_{66} + a_{33}a_{44}a_{66} + a_{11}a_{66}a_{77} + a_{22}a_{55}a_{77} + a_{33}a_{44}a_{77}\\
&+ a_{33}a_{55}a_{66} + a_{22}a_{66}a_{77} + a_{33}a_{55}a_{77} + a_{44}a_{55}a_{66} + a_{33}a_{66}a_{77}\\
&+ a_{44}a_{55}a_{77} + a_{44}a_{66}a_{77} + a_{55}a_{66}a_{77}, a_{13}a_{32} - a_{11}a_{33} - a_{11}a_{22} - a_{11}a_{44} - a_{22}a_{33} + a_{14}a_{42} - a_{11}a_{55}\\
&- a_{22}a_{44} - a_{11}a_{66} - a_{22}a_{55} - a_{33}a_{44} - a_{11}a_{77}\\
&- a_{22}a_{66} - a_{33}a_{55} - a_{22}a_{77} - a_{33}a_{66} - a_{44}a_{55} - a_{33}a_{77} - a_{44}a_{66} - a_{44}a_{77} - a_{55}a_{66}\\
&- a_{55}a_{77} - a_{66}a_{77}, a_{11} + a_{22} + a_{33} + a_{44} + a_{55} + a_{66} + a_{77}]
\end{aligned}
$$

References

[1] Spanish Flu: Death toll. https://en.wikipedia.org/wiki/Spanish_flu.

[2] Spanish Flu: GDP loss. https://www.encyclopedie-environnement.org/en/health/viral-pandemics-of-the-modern-era/#:~:text=Viral%20pandemics%20of%20the%20modern%20era%20(1918%20to%20the%20present,%2C%20SARS%2DCoV%2D2.&text=The%20Mexican%20swine%20flu%20(Influenza,H1N1%20virus)%202009%2D2010.

[3] HIV/AIDS epidemic https://en.wikipedia.org/wiki/Epidemiology_of_HIV/AIDS.

[4] World Health Organization (WHO) website, Small-pox: https://www.who.int/csr/disease/smallpox/vaccines/en/.

[5] COVID-19 cases: Global count. https://www.worldometers.info/coronavirus/?fbclid=IwAR35ZFiRZJ8tyBCwazX2N-k7yJjZOLDQiZSA_MsJAfdK74s8f2a_Dgx4iVk.

[6] Ochoche JM, Gweryina RI. A mathematical model of measels with vaccination and two phases of infectiousness. IOSR J Math 2014;10:95–105. http://dx.doi.org/10.9790/5728-101495105.

[7] Prosper O, Saucedo O, Thompson D, Garcia GT, Wang Z. Vaccination strategy and optimal control for seasonal and H1N1 influenza outbreak. Math Biosci Eng 2011;8(1):141–70. http://dx.doi.org/10.3934/mbe.2011.8.141.

[8] Raza A, Chu YM, Bajuri MY, Ahmadian A, Ahmed N, Rafiq M, Salahshour S. Dynamical and nonstandard computational analysis of heroin epidemic model. Results Phys 2022;34:105245. http://dx.doi.org/10.1016/j.rinp.2022.105245.

[9] Shen WY, Chu YM, Rahman Mur, Mahariq I, Zeb A. Mathematical analysis of HBV and HCV co-infection model under nonsingular fractional order derivative. Results Phys 2021;28:104582. http://dx.doi.org/10.1016/j.rinp.2021.104582.

[10] Chen SB, Rajaee F, Yousefpour A, Alcaraz R, Chu YM, Gómez-Aguilar JF, Bekiros S, Aly AA, Jahanshahi H. Antiretroviral therapy of HIV infection using a novel optimal type-2 fuzzy control strategy. Alex Eng J 2021;60(1):1545–55. http://dx.doi.org/10.1016/j.aej.2020.11.009.

[11] Hoan LVC, Akinlar MA, Inc M, Gómez-Aguilar JF, Chu YM, Almohsen B. A new fractional-order compartmental disease model. Alex Eng J 2020;59(5):3187–96. http://dx.doi.org/10.1016/j.aej.2020.07.040.

[12] Gul N, Bilal R, Algehyne EA, Alshehri MG, Khan MA, Chu YM, S. Islam. The dynamics of fractional order Hepatitis B virus model with asymptomatic carriers. Alex Eng J 2021;60(4):3945–55. http://dx.doi.org/10.1016/j.aej.2021.02.057.

[13] Chu YM, Khan MF, Ullah S, Shah SAA, Farooq M, bin Mamat M. Mathematical assessment of a fractional-order vector–host disease model with the Caputo–Fabrizio derivative. Math Methods Appl Sci 2022. http://dx.doi.org/10.1002/mma.8507.

[14] Ngonghala CN, Iboi E, Eikenberry S, Scoth M, MacIntyre RC, Bonds MH, Gumel AB. Mathematical assessment of the impact of non-pharmaceutical interventions on curtailing the 2019 novel Coronavirus. Math Biosci 2020;325:108364. http://dx.doi.org/10.1016/j.mbs.2020.108364.

[15] Tang B, Wang X, et al. Estimation of the transmission risk of the 2019-nCoV and its implication for public health interventions. J Clin Med 2020;9:462. http://dx.doi.org/10.3390/jcm9020462.

[16] Fanelli D, Piazza F. Analysis and forecast of COVID-19 spreading in China, Italy and France. Chaos Solitons Fractals 2020;138:1–5. http://dx.doi.org/10.1016/j.chaos.2020.109761.

[17] Pang L, Liu S, Zhang X, Tian T, Zhao Z. Transmission dynamics and control strategies of COVID-19 Wuhan, China. J Biol Systems 2020;28(3):1–18. http://dx.doi.org/10.1142/S0218339020500096.

[18] Li MT, Sun GQ, Zhang J, Zhao Y, Pei X, Li L, et al. Analysis of COVID-19 transmission in Shanxi Province with discrete time imported cases. Math Biosci Eng 2020;17:3710–20. http://dx.doi.org/10.3934/mbe.2020208.

[19] Sarkar K, Khajanchi S, Nieto J. Modeling and forecasting the COVID-19 pandemic in India. Chaos Solitons Fractals 2020;139:110049. http://dx.doi.org/10.1016/j.chaos.2020.110049.

[20] Khajanchi S, Sarkar K, Mondal J, Nisar KS, Abdelwahab SF. Mathematical modeling of the COVID-19 pandemic with intervention strategies. Results Phys 2021;25:104285. http://dx.doi.org/10.1016/j.rinp.2021.104285.

[21] Youssef H, Alghamdi N, Ezzat MA, El-Bary AA, Shawky AM. Study on the SEIQR model and applying the epidemiological rates of COVID-19 epidemic spread in Saudi Arabia. Infect Dis Model 2021;6:678–92. http://dx.doi.org/10.1016/j.idm.2021.04.005.

[22] Das DK, Khatua A, Kar TK, Jana S. The effectiveness of contact tracing in mitigating COVID-19 outbreak: A model-based analysis in the context of India. Appl Math Comput 2021;404:126207. http://dx.doi.org/10.1016/j.amc.2021.126207.

[23] Garba SM, Lubuma JM, Tsanou B. Modeling the transmission dynamics of the COVID-19 pandemic in South Africa. Math Biosci 2020;108441. http://dx.doi.org/10.1016/j.mbs.2020.108441.

[24] Acuna-Zegarra MA, Santana-Cibrian M, Velasco-Hernandez JX. Modeling behavioral change and COVID-19 containment in Mexico: A trade-off between lockdown and compliance. Math Biosci 2020;108370. http://dx.doi.org/10.1016/j.mbs.2020.108370.

[25] Sardar T, Nadim SS, Rana S, Chattopadhyay J. Assessment of lockdown effect in some states and overall India: A predictive mathematical study on COVID-19 outbreak. Chaos Solitons Fractals 2020;139:110078. http://dx.doi.org/10.1016/j.chaos.2020.110078.

[26] Rohith G, Devika KB. Dynamics and control of COVID-19 pandemic with nonlinear incidence rates. Nonlinear Dynam 2020;101. http://dx.doi.org/10.1007/s11071-02005774-5, 2013-1026.

[27] Sinha AK, Namdev N, Shende P. Mathematical modeling of the outbreak of COVID-19. Netw Model Anal Health Inform Bioinform 2022;11:5. http://dx.doi.org/10.1007/s13721-021-00350-2.

[28] Khan MA, Atangana A. Mathematical modeling and analysis of COVID-19: A study of new variant Omicron. Physica A 2022;599:127452. http://dx.doi.org/10.1016/j.physa.2022.127452.

[29] Premarathna IHK, Srivastava HM, Juman ZAMS, AlArjani A, Uddin MS, Sana SS. Mathematical modeling approach to predict COVID-19 infected people in Sri Lanka. AIMS Math 2021;7(3):4672–99, https://www.aimspress.com/article/doi/10.3934/math.2022260.

[30] Kamrujjaman M, Saha P, Islam MS, Ghosh U. Dynamics of SEIR model: A case study of COVID-19 in Italy. Results Control Optim 2022;7:100119. http://dx.doi.org/10.1016/j.rico.2022.100119.

[31] Zhao TH, Castillo O, Jahanshahi H, Yusuf A, Alassafi MO, Alsaadi FE, Chu YM. A fuzzy-based strategy to suppress the novel coronavirus (2019-NCOV) massive outbreak. Appl Comput Math 2021;20(1):160–76.

[32] Pandey P, Chu YM, Gómez-Aguilar JF, Jahanshahi H, Aly AA. A novel fractional mathematical model of COVID-19 epidemic considering quarantine and latent time. Results Phys 2021;26:104286. http://dx.doi.org/10.1016/j.rinp.2021.104286.

[33] Chu YM, Ali A, Khan MA, Islam S, Ullah S. Dynamics of fractional order COVID-19 model with a case study of Saudi Arabia. Results Phys 2021;21:103787. http://dx.doi.org/10.1016/j.rinp.2020.103787.

[34] Shen ZH, Chu YM, Khan MA, Muhammad S, Al-Hartomy OA, Higazy M. Mathematical modeling and optimal control of the COVID-19 dynamics. Results Phys 2021;31:105028. http://dx.doi.org/10.1016/j.rinp.2021.105028.

[35] Nath BJ, Dehingia K, Mishra VN, Chu YM, Sarmah HK. Mathematical analysis of a within-host model of SARS-CoV-2. Adv Difference Equ 2021;1:1–11. http://dx.doi.org/10.1186/s13662-021-03276-1.

[36] Vales EA, Perez AGC. Dynamics of a time-delayed SIR epidemic model with logstic growth and saturayed treatment. Chaos Solitons Fractals 2019;127:5–69. http://dx.doi.org/10.1016/j.chaos.2019.06.024.

[37] Kumar A, Nilam. Stability of a time delayed SIR epidemic model along with nonlinear incidence rate and holling type-ii treatment rate. Int J Comput Methods 2018;15(6):1850055. http://dx.doi.org/10.1142/S021987621850055X.

[38] Liu X, Long X, Zheng X, Meng G, Balachandran B. Spatial–temporal dynamics of a drill string with complex time-delay effects: bit bounce and stick–slip oscillations. Int J Mech Sci 2020;170:105338. http://dx.doi.org/10.1016/j.ijmecsci.2019.105338.

[39] Liu Z, Magal P, Seydi O, Webb G. A COVID-19 epidemic model with latency period. Infect Dis Model 2020;5:323–37. http://dx.doi.org/10.1016/j.idm.2020.03.003.

[40] Liu X, Zheng X, Balachandran B. COVID-19: data-driven dynamics, statistical and distributed delay models, and observations. Nonlinear Dynam 2020;101:1527–43. http://dx.doi.org/10.1007/s11071-020-05863-5.

[41] Rihan FA, Alsakaji HJ, Rajivganthi C. Stochastic SIRC epidemic model with time-delay for COVID-19. Adv Differ Equ 2020;502. http://dx.doi.org/10.1186/s13662-020-02964-8.

[42] Adhikary A, Pal A. A six compartments with time-delay model SHIQRD for the COVID-19 pandemic in India: During lockdown and beyond. Alex Eng J 2022;61:1403–12. http://dx.doi.org/10.1016/j.aej.2021.06.027.

[43] Nastasi G, Perrone C, Taffara S, Vitanza G. A time-delayed deterministic model for the spread of COVID-19 with calibration on a real dataset. Mathematics 2022;10:661. http://dx.doi.org/10.3390/math10040661.

[44] Raza A, Ahmadian A, Rafiq M, Ang MC, Salahsour S, Pakdaman M. The impact of delay stratergies on the dynamics of coronavirus pandemic model with nonlinear incidence rate. Fractals 2022;30(5):2240121. http://dx.doi.org/10.1142/S0218348X22401211.

[45] Shan HS, Lee J, Langworthy B, Xin J, James P, Yang Y, Wang M. Delay in the effect of restricting community mobility on the spread of COVID-19 during the first wave in the United States. 2022;9(1):0fab586. http://dx.doi.org/10.1093/ofid/ofab586.

[46] Tang B, Bragazzi NL, et al. An updated estimation of the risk of transmission of the novel coronavirus (2019-nCov). Infect Dis Model 2020;5:248–55. http://dx.doi.org/10.1016/j.idm.2020.02.001.

[47] Khatua D, De A, et al. A dynamic optimal control model for SARS-CoV-2 in India. SSRN Electron J 2020. http://dx.doi.org/10.2139/ssrn.3597498.

[48] Shah NH, Suthar AH, Jayswal EN. Control strategies to curtail transmission of COVID-19. Int J Math Math Sci 2020;2020:2649514. http://dx.doi.org/10.1155/2020/2649514.

[49] Moore SE, Okyere E. Controlling the transmission dynamics of COVID-19. 2020, https://arxiv.org/abs/2004.00443.

[50] Kouidere A, Khajji B, et al. A mathematical modelling with optimal control strategy of transmission of Covid-19 pandemic virus. Commun Math Biol Neurosci Commun Math Biol Neurosci 2020;2020:24. http://dx.doi.org/10.28919/cmbn/4599.

[51] Zamir M, Shah Z, Nadeem F, Memood A, Alrabaiha H, Kumam P. Non pharmaceutical interventions for optimal control of COVID-19. Comput Methods Programs Biomed 2020;196:105642. http://dx.doi.org/10.1016/j.cmpb.2020.105642.

[52] Yousefpour A, Jahanshahi H, Bekiros S. Optimal policies for control of the novel coronavirus disease (COVID-19) outbreak. Chaos Solitons Fractals 2020;136:109883. http://dx.doi.org/10.1016/j.chaos.2020.109883.

[53] Araz SI. Analysis of a Covid-19 model: Optimal control, stability and simulations. Alex Eng J 2020;60(1):647–58. http://dx.doi.org/10.1016/j.aej.2020.09.058.

[54] Obsu LL, Balcha SF. Optimal control strategies for the transmission risk of COVID-19. J Biol Dyn 2020;14(1):590–607. http://dx.doi.org/10.1080/17513758.2020.1788182.

[55] Sasmita NR, Ikhwan M, Suyanto S, et al. Optimal control on a mathematical model to pattern the progression of coronavirus disease 2019 (COVID-19) in Indonesia. Glob Health Res Policy 2020;38. http://dx.doi.org/10.1186/s41256-020-00163-2.

[56] Mandal M, Jana S, Nandi SK, Khatua A, Adak S, Kar TK. A model based study on the dynamics of COVID-19: Prediction and control. Chaos Solitons Fractals 2020;136:109889. http://dx.doi.org/10.1016/j.chaos.2020.109889.

[57] Khan AA, Ullah S, Amin R. Optimal control analysis of COVID-19 vaccine epidemic model: a case study. Eur Phys J Plus 2022;137:156. http://dx.doi.org/10.1140/epjp/s13360-022-02365-8.

[58] Kumar RP, Basu S, Santra PK, Ghosh D, Mahapatra GS. Optimal control design incorporating vaccination and treatment on six compartment pandemic dynamical system. Results Control Optim 2022;7:100115. http://dx.doi.org/10.1016/j.rico.2022.100115.

[59] Chang X, Liu M, Jin Z, Wang J. Studying on the impact of media coverage on the spread of COVID-19 in Hubei Province, China. Math Biosci Eng 2020;17(4):3147–59. http://dx.doi.org/10.3934/mbe.2020178.

[60] Yang C, Wang J. A mathematical model for the novel coronavirus epidemic in Wuhan, China. Math Biosci Eng 2020;17(3):2708–24. http://dx.doi.org/10.3934/mbe.2020148.

[61] Re-appearance of COVID-19 symptoms (China), Los Angeles Times: https://www.latimes.com/world-nation/story/2020-03-13/china-japan-korea-coronavirus-reinfection-test-positive#:~:text=Dale%20Fisher%2C%20professor%20of%20medicine,on%20discharged%20cases%20in%20China.

[62] Re-appearance of COVID-19 symptoms (Hong Kong): https://www.wsj.com/articles/researchers-report-covid-19-reinfection-in-hong-kong-11598295631.

[63] Kumar A, Rathi N. Stability of a delayed SIR epidemic model by introducing two explicit treatment classes along with nonlinear incidence rate and Holling type treatment. Comput Appl Math 2019;38:130. http://dx.doi.org/10.1007/s40314-019-0866-9.

[64] Kumar A, Rathi N, Goel K. Nonlinear dynamics of a time-delayed epidemic model with two explicit aware classes, saturated incidences, and treatment. Nonlinear Dynam 2020;101:1693–715. http://dx.doi.org/10.1007/s11071-020-05762-9.

[65] Kumar A, Rathi N, Goel K. A deterministic time-delayed SIR epidemic model: Mathematical modelling and analysis. Theory Biosci 2020;139:67–76. http://dx.doi.org/10.1007/s12064-019-00300-7.

[66] Bhatia SK, Chauhan S, Maheshwari P. Sirs model with double time delay. Indian J Ind Appl Math 2016;7(2):244–61. http://dx.doi.org/10.5958/1945-919X.2016.00021.9.

[67] Capasso V, Serio G. A generalization of the Kermack C Mckendrick deterministic epidemic model. Math Biosci 1978;42(1–2):41–61. http://dx.doi.org/10.1016/0025-5564(78)90006-8.

[68] Zaki Nazar, Mohamed Elfadil A. The estimations of the COVID-19 incubation period: A scoping reviews of the literature. J Infect Public Health 2021;14:638–46. http://dx.doi.org/10.1016/j.jiph.2021.01.019.

[69] Qin J, You C, Lin Q, Hu T, Yu S, Zhou X-H. Estimation of incubation period distribution of COVID-19 using disease onset forward time: A novel cross-sectional and forward followup study. Sci Adv 2020;6:eabc1202. http://dx.doi.org/10.1126/sciadv.abc1202.

[70] Backer Jantien A, Don Klinkenberg, Jacco Wallinga. Incubation period of 2019 novel coronavirus (2019-nCoV) infections among travellers from Wuhan, China. 20–28 2020. Euro Surveill 2020;25(5):2000062. http://dx.doi.org/10.2807/1560-7917.ES.2020.25.5.2000062.

[71] COVID-19 Incubation Period https://www.worldometers.info/coronavirus/coronavirus-incubation-period/.

[72] Lauer SA, Grantz KH, Bi Q, Jones FK, Zheng Q, Meredith HR, Azman AS, Reich NG, Lessler J. The incubation period of coronavirus disease 2019 (COVID-19) from publicly reported confirmed cases: Estimation and application. Ann Intern Med 2020;172(9):577–82. http://dx.doi.org/10.7326/M20-0504.

[73] Quesada JA, López-Pineda A, Gil-Guillén VF, Arriero-Marín JM, Gutiérrez F, CarratalaMunuera C. Período de incubación de la COVID-19: revisión sistemática y metaanálisis incubation period of COVID-19: A systematic review and meta-analysis. Rev Clin Esp(Barc) 2021;221(2):109–17. http://dx.doi.org/10.1016/j.rce.2020.08.005.

[74] Naresh R, Tripathi A, Tchuenche JM, Sharma D. Stability analysis of a time delayed SIR epidemic model with nonlinear incidence rate. Comput Math Appl 2009;58:348–59. http://dx.doi.org/10.1016/j.camwa.2009.03.110.

[75] Birkhoff G, Rota GC. Ordinary differential equations. Boston: Ginn; 1982.

[76] Kassa SM, Njagarah HJB, Terefe YA. Analysis of the mitigation strategies for COVID-19: from mathematical modelling perspective. Chaos Solitons Fractals 2020;138:109968. http://dx.doi.org/10.1016/j.chaos.2020.109968.

[77] Bugalia Sarita, Tripathi Jai Prakash, Wang Hao. Mathematical modeling of intervention and low medical resource availability with delays: Applications to COVID-19 outbreaks in Spain and Italy. 2021;18(5):5865-920. http://dx.doi.org/10.3934/mbe.2021295.
[78] Tipsri S, Chinviriyasit W. Stability analysis of SEIR model with saturated incidence and time delay. Int J Appl Phys Math 2014;4:42–5. http://dx.doi.org/10.7763/IJAPM.2014.V4.252.
[79] Mukandavire Z, Garira W, Chiyaka C. Asymptotic properties of an HIV/AIDS model with a time delay. J Math Anal Appl 2007;330(2):916–33. http://dx.doi.org/10.1016/j.jmaa.2006.07.102.
[80] Samsuzzoha M, Singh M, Lucy D. Uncertainty and sensitivity analysis of the basic reproduction number of a vaccinated epidemic model of influenza. Appl Math Model 2013;37(3):903–15. http://dx.doi.org/10.1016/j.apm.2012.03.029.
[81] Zaman G, Kang YH, Jung IH. Optimal treatment of an SIR epidemic model with time delay. Biosystems 2009;98(1):43–50. http://dx.doi.org/10.1016/j.biosystems.2009.05.006.
[82] Lukes DL. Differential equations: Classical to controlled, mathematics in science and engineering. New York: Academic Press; 1982.
[83] Abta A, Laarabi H, Alaoui HM, Zhang C. The hopf bifurcation analysis and optimal control of a delayed SIR epidemic mode. Int J Anal 2014;2014:940819. http://dx.doi.org/10.1155/2014/940819.
[84] Zhu Q, Yang X, Yang L, Zhang C. Optimal control of computer virus under a delayed model. Appl Math Comput 2012;218(23):11613–9. http://dx.doi.org/10.1016/j.amc.2012.04.092.
[85] Li Q, Guan X, Wu P, Wang X, Zhou L, Tong Y, Ren R, Leung KSM, Lau EHY, Wong JY, Xing X, Xiang N, et al. Early transmission dynamics in Wuhan, China, of novel coronavirus–Infected pneumonia. N Engl J Med 2020;382:1199–207. http://dx.doi.org/10.1056/NEJMoa2001316, nejm.org/doi/10.1056/NEJMoa2001316#article_citing_articles.
[86] Huang C, Wang Y, Li X, Ren L, Zhao J, Hu Y, et al. Clinical features of patients infected with 2019 novel coronavirus in Wuhan, China. Lancet 2020;395:497–506. http://dx.doi.org/10.1016/S0140-6736(20)30183-5.
[87] Zhao S, Lin Q, Ran J, Musa SS, Yang G, Wang W, Lou Y, Gao D, Yang L, He D, Wang MH. Preliminary estimation of the basic reproduction number of novel coronavirus (2019-nCoV) in China, from 2019 to 2020: A data- driven analysis in the early phase of the outbreak. Int J Infect Dis 2020;92:214–7. http://dx.doi.org/10.1016/j.ijid.2020.01.050.
[88] Billah MA, Miah MM, Khan MN. Reproductive number of coronavirus: A systematic review and meta-analysis based on global level evidence. PLOS ONE 2020;15(11):e0242128. http://dx.doi.org/10.1371/journal.pone.0242128.
[89] Shao N, Cheng J, Chen W. The reproductive number R0 of COVID-19 based on estimate of a statistical time delay dynamical system. MedRxiv 2020. http://dx.doi.org/10.1101/2020.02.17.20023747.
[90] Yu CJ, Wang ZX, Yue X, Hu MX, Chen K, Qin G. Assessment of basic reproductive number for COVID-19 at global level. PubMed 2020;100(18):e25837. http://dx.doi.org/10.1097/MD.0000000000025837.
[91] Mishra AM, Purohit SD, Owolabi KM, Sharma YD. A nonlinear epidemiological model considering asymptotic and quarantine classes for SARS CoV-2 virus. Chaos Solitons Fractals 2020;138:109953. http://dx.doi.org/10.1016/j.chaos.2020.109953.
[92] Active Cases in China: https://www.worldometers.info/coronavirus/country/china/.